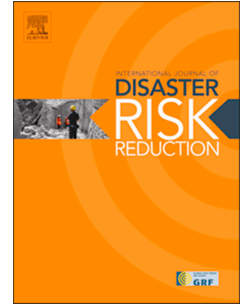


Journal Pre-proof

Resilient communities through safer schools

Dina D'Ayala, Carmine Galasso, Arash Nassirpour, Rohit Kumar Adhikari, Luis Yamin, Rafael Fernandez, Dexter Lo, Lessandro Garciano, Andres Oreta



PII: S2212-4209(19)30930-6

DOI: <https://doi.org/10.1016/j.ijdr.2019.101446>

Reference: IJDRR 101446

To appear in: *International Journal of Disaster Risk Reduction*

Received Date: 13 July 2019

Revised Date: 9 December 2019

Accepted Date: 11 December 2019

Please cite this article as: D. D'Ayala, C. Galasso, A. Nassirpour, R.K. Adhikari, L. Yamin, R. Fernandez, D. Lo, L. Garciano, A. Oreta, Resilient communities through safer schools, *International Journal of Disaster Risk Reduction* (2020), doi: <https://doi.org/10.1016/j.ijdr.2019.101446>.

This is a PDF file of an article that has undergone enhancements after acceptance, such as the addition of a cover page and metadata, and formatting for readability, but it is not yet the definitive version of record. This version will undergo additional copyediting, typesetting and review before it is published in its final form, but we are providing this version to give early visibility of the article. Please note that, during the production process, errors may be discovered which could affect the content, and all legal disclaimers that apply to the journal pertain.

© 2019 Published by Elsevier Ltd.

Resilient communities through safer schools

Dina D'Ayala¹, Carmine Galasso¹, Arash Nassirpour¹, Rohit Kumar Adhikari¹, Luis Yamin², Rafael Fernandez², Dexter Lo³, Lessandro Garciano⁴, Andres Oreta⁴

EPICentre, University College London, UK
Universidad de los Andes, Bogota', Columbia
Xavier University, Cagayan de Oro, Philippines
De La Salle University, Manila, Philippines

Abstract

Access to education is a basic human right. It is the 4th of the 17 *Sustainable Development Goals* (SDGs) and education is strongly associated with poverty reduction. Providing facilities to educate children requires construction of school buildings and rapid expansion of curricula. However, in the rush to fulfil the right to education, are children being put at risk? What attention is being given to structural safety during the construction of new school facilities? The growing consensus among stakeholders is that public school infrastructure in developing countries worldwide is particularly susceptible to natural hazards. This highlights a compelling need for developing and implementing effective, integrated, and 'ground-real' strategies for assessing and radically improving the safety and resilience of schools across those countries.

To this aim, the paper explores two main issues: effectiveness at scale and the relevance of multiple hazard effects on the resilience of school infrastructure. Specifically, the paper first discusses the challenges associated with the World Bank Global Program for Safer School (GPSS) and the development of its Global Library of School Infrastructure (GLOSI), highlighting the issues associated with producing a tool which can be effective at scale and support nationwide risk models for school infrastructure across the world, so that fairness and relevance of investment can be achieved. This is followed by the illustration of a number of specific tools developed by the authors to expand the risk prioritization procedures used for seismic hazard, to other hazards such as flood and windstorm and to quantify the reduction in seismic fragility obtained by implementing specific strengthening strategies. Rapid visual survey forms, a mobile app, a multi-hazard risk prioritization ranking, and numerical fragility relationships are presented and their application discussed in relation to a case study in the Philippines. The proposed tools represent a first step toward a detailed multi-hazard risk and resilience assessment framework of school infrastructure. The aim is to allow stakeholders and decision-makers to quickly identify the most vulnerable structures among the surveyed stock, to guide more detailed data collection campaigns and structural assessment procedures, such as analytical vulnerability approaches, and ultimately to plan further retrofitting/strengthening measures or, if necessary, school replacement/relocation.

1. Introduction

The last decade has seen numerous reports of casualties of school children in school building collapses caused by natural hazards. In 2008, the Wenchuan earthquake caused the collapse of over 7,000 schoolrooms, mostly in rural areas, reportedly leading to the death of over 5,000 students (though some parents believe the real figure is twice that officially cited) and the injury of over 15,000 students (The Guardian, 2009). This situation is not an exception – each year natural hazards around the world have had devastating effects on children's education. Typhoon Haiyan damaged more than 2,500 schools and affected 1.4 million children in the Philippines in 2013 (ACAPS, 2014). In 2016, recovery of education facility was far from complete (IFRC, 2016). When an M7.8 earthquake struck the Gorkha region, Nepal, on April 25, 2015, more than 7,000 school buildings were collapsed or significantly damaged (NPC, 2015). The massive disruption caused by the earthquake and its aftershocks on school infrastructure has reverberated into children's development. The National Reconstruction Authority (NRA, 2018) reports that at the end of 2018 "... 80% progress has been made in the reconstruction of educational institutions". Out of the 7,553 damaged schools, 55% have been reconstructed while 25% are under construction, hampering children education and development for several years. An assessment of schools after the M7.3 Ezgeleh, Iran earthquake of November 12, 2017, show that 89% of all the school buildings in the affected area, passed the level of Immediate Occupancy (IO). The majority of the damaged schools are unreinforced masonry (URM) building with no confinement, which date back to more than 30 years ago (DRES, 2017). The Central Sulawesi earthquake of September 2018 in Indonesia caused heavy damage or collapse of more than 1500

57 schools affecting 184,000 pupils (UNICEF, 2018). Reconnaissance survey identified confined masonry
58 school buildings in Palu and nearby regions as particularly affected, while most of the reinforced concrete
59 school buildings survived without any damage (Lagesse et al., 2019). The recent cyclone Idai that hit South
60 East Africa in April 2019 caused massive devastation and flooding in Mozambique, Zimbabwe and Malawi.
61 It is estimated that thousands of classrooms were damaged or destroyed and half a million children have had
62 their education disrupted (Watt, 2019).

63 School buildings vulnerability and damage due to disastrous natural-hazard events is clearly a global
64 problem and one that it is not reducing in size. Schools play a critical role in the education of a community's
65 next generation; school children are amongst the most vulnerable components of society due to their age and
66 their developmental stage. A safer and resilient school can save children lives, provide a safe haven for the
67 local community, serving as a temporary shelter and helping to bring normalcy back to society in times of
68 disaster. However, public school buildings constructed prior to adequate building codes, often have structural
69 deficiencies which are heightened by their architectural configuration due to the specific use requirements.
70 The above considerations clearly identify the need for prioritizing school building physical vulnerability
71 assessment and allocate resources for retrofitting/strengthening plans.

72 It was indeed the extensive loss of school children's lives in the 2008 Wenchuan earthquake that triggered
73 the resolution, promulgated during the 2009 session of the Global Platform for Disaster Risk Reduction,
74 committing governments to "*innovation and education to build a culture of safety and resilience at all*
75 *levels*" (GDPRR, 2009; IISD, 2009). The participating governments also committed to:

- 76 • national assessments of the safety of existing education and health facilities to be undertaken by
77 2011;
- 78 • concrete action plans for safer schools and hospitals to be developed and implemented by 2015 in all
79 disaster-prone countries.

80 These two resolutions, in turn, stimulated efforts to develop a Comprehensive School Safety (CSS)
81 framework, elaborated by Save the Children in coordination with the Global Alliance for Disaster Risk
82 Reduction and Resilience in the Education Sector (GADRRRES), set up in 2013, with an important emphasis
83 shift from disaster recovery to disaster preparedness and prevention. The International Finance Corporation
84 (IFC) published a "Disaster and Emergency Preparedness: Guidance for Schools" (ICF, 2010), focussed on
85 multiple hazards, which, following a three prongs approach, including building safety, community safety and
86 education preparedness, anticipated the CSS framework.

87 The Comprehensive School Safety Framework, updated in 2017, is built on three pillars: Safe Learning
88 Facilities; School Disaster Management; Risk Education and Resilience Education. The CSS framework is
89 intended to promote school safety as a priority area for sustainable development, risk reduction and
90 resilience, with a strong emphasis on the need for multi-hazard risk assessment and mitigation of the existing
91 school infrastructure (UNISDR, 2014).

92 Concurrently, the Worldwide Initiative for Safe Schools (WISS, 2013), is a government-led global
93 partnership for advancing safe school implementation at the national level, currently coordinated by the UN
94 Office for Disaster Risk Reduction (UNDRR) to promote key safe school initiatives in support of resilient
95 educational facilities, school disaster management, disaster risk reduction and resilience education. The
96 WISS was endorsed by GADRRRES members and resulted in the political commitment of 21 "Safe School
97 Leader" countries to implement school safety on the ground. These are mainly countries receivers of Official
98 Development Assistance (ODA) by the Development Assistance Committee (DAC) of the Organisation for
99 Economic Co-operation and Development (OECD).

100 The OECD has produced policy guidance on "Protecting students and schools from earthquakes"
101 summarised in the seven OECD principles for school seismic safety (OECD, 2017). The seven principles
102 encompass seismic safety policy, including financial and human resources to ensure implementation,
103 accountability, building codes, training and qualification, preparedness and planning, community awareness,
104 and risk reduction. While substantial improvement has been achieved since its first publication in 2005, only
105 20 nations worldwide have subscribed to it, none being an ODA country.

106 The initiatives outlined above align well with the "*Substantial reduction of disaster damage to critical*
107 *infrastructure, [...], among them educational facilities...*" advocated as one of the seven global targets of the
108 Sendai Framework on Disaster Risk Reduction 2015-2030 (UNDRR, 2015). The need to improve the
109 resilience of school infrastructure in ODA countries is paramount, heightened by growing urbanization, rapid

110 increase of poorly built infrastructure and uncontrolled land development, increasing exposure and
111 vulnerability of populations to natural hazards.

112 The development of safer school facilities is critical as access to education is a fundamental human right and
113 underpins any other development goal. Better education is also a fundamental driver of poverty reduction.
114 However, providing education facilities for all requires rapid expansion and delivery of school building
115 programs, nationally and internationally. In the rush to fulfil the right to education, *are children being put at*
116 *risk? What attention is paid to the hazard resilience of this new educational infrastructure?* There is a
117 compelling need to develop and implement effective, intergraded, and 'ground-real' strategies for assessing
118 and radically improving the safety and resilience of existing and new built schools. The World Bank (WB)
119 and other international financial institutions have large and diverse investment portfolios on school
120 infrastructure in different parts of the world, amounting to billions of US\$. However, these programmes
121 cannot fulfil by 2030 the education infrastructure gap with new facilities only. Therefore, there is an urgent
122 need to develop risk and resilience assessment and risk mitigation strategies suitable to different construction
123 types in different countries, exposed to different hazards.

124 The delivery of such global programmes for school safety requires a clear baseline against which to
125 benchmark exiting school infrastructure in different geographical context and a clear framework of
126 performance target that new construction and retrofitting of existing school should achieve. To this aim, the
127 Global Program for Safer Schools (GPSS) aims to boost and facilitate informed, large-scale investments for
128 the safety and resilience of new and existing school infrastructure at risk from natural hazards, contributing
129 to high-quality learning environments. The focus is primarily on public school infrastructure in developing
130 countries (The World Bank, 2019).

131 The GPSS focuses on delivering the first of the three pillars of the CSS framework (UNDRR, 2017). At the
132 global level, the program focuses on generating evidence-based knowledge and making it available
133 worldwide to promote and facilitate a long-term and systematic approach to improving the safety of school
134 infrastructure at scale, using quantitative risk assessments. At the country level, the program supports -
135 through WB technical assistance projects - governments' efforts to: design and implementation of safer
136 school programs; influence policy reforms and wider investments in risk reduction to create safer school
137 environments; inform long-term national strategies to prioritize safety at scale and build continuity across
138 investment and programme deliveries.

139 The inclusion of school infrastructure resilience as one of the main targets of the Sendai framework has
140 sparked in the last five years renewed impetuous in this sector and, besides the World Bank, most regional
141 development banks and aid agencies have launched programmes of technical assistance to move the agenda
142 forward. This has also resulted in a renewed interest on the part of the scientific community, leading to
143 several bilateral or multilateral knowledge exchange and development project.

144 The authors have directly contributed to research and development in this sector in the past three years, as
145 World Bank scientific advisors and partners in the delivery of the GPSS and as principal investigators in a
146 number of collaborative projects sponsored by the UK Research Councils. The paper first presents the efforts
147 within the GPSS to deliver a global repository for school buildings vulnerability. The structure of the
148 repository and the methodology used to derive consistent vulnerability functions for several typologies of
149 school buildings exposed to seismic hazard are reported and illustrated by way of an example. The second
150 part of the paper shows how this approach can be expanded and extended to include other hazard
151 vulnerability by way of application to the school infrastructure in the Philippines.

152

153

154 2. The World Bank GLOSI initiative: development of a global repository of school building 155 vulnerability functions

156 The Global Facility for Disaster Reduction and Recovery (GFDRR) launched the GPSS in 2014 with a focus
157 on integrating risk considerations into education infrastructure investments. The GPSS has the following
158 three main goals:

- 159 • Facilitate and inform production of consistent evidence-based knowledge on safety and
160 resilience of school infrastructure worldwide. As a result, it will facilitate exchange of

- 161 information among different countries, and build efficiency in the implementation of safer
162 school projects across the world both in pre- and post-disaster contexts;
- 163 • Inform the implementation of technical solutions to improve the safety of school
164 infrastructure at scale based on past experiences and innovation, and open opportunities to
165 adapt them to local contexts; and
 - 166 • Build efficiency on the implementation of investments for vulnerability reduction of school
167 infrastructure by establishing consistent prioritization and optimization methodologies.

168 The delivery of the first of these goals requires several specific actions: the first is to formulate a
169 methodology for structural classification of school infrastructure, along with a consistent taxonomy, that can
170 be used worldwide. Once, such classification system is developed, then a comprehensive database with
171 construction and vulnerability information on the most common structural typologies of school infrastructure
172 in developing countries at risk from natural hazards can be established. This can be built upon as school
173 infrastructure development programmes are implemented across the world and assessment and retrofit
174 campaigns multiply. The setting up of such a database allows to identify similarity and differences among
175 regions in terms of materials, construction technology and vulnerability in school infrastructure, and the
176 study of such parameters supports the development of a repository of fragility (likelihood of physical damage
177 as a function of a hazard intensity measure) and vulnerability (likelihood of economic loss as a function of a
178 hazard intensity measure) functions for each structural typology. This is a critical component of any risk
179 assessment exercise, whether at local, national or at regional scale, an essential step to determine
180 prioritization and optimization strategies for investments to realise the GPSS.

181 The World Bank has partnered with University College London (UCL), UK, and University of Los Andes,
182 Colombia, to establish a working group to develop the Global Library of School Infrastructure (GLOSI) (The
183 World Bank, 2019), which underpins the first pillar of the GPSS. To provide context to the GLOSI work the
184 next section presents a review of building classification systems and their limitation of applicability to
185 schools. The following sections present the GLOSI Taxonomy, the methodology to identify index buildings,
186 and the methodology applied to derive fragility and vulnerability functions.

187

188 **2.1. Review of Existing Building Classification Systems and Rapid Visual Screening Methods**

189 For the purpose of determining seismic risk of the built environment, several building classification systems
190 are available, although only few have been developed considering global construction types and hence
191 globally applicable (e.g., Coburn and Spence, 2002; Jaiswal and Wald, 2008; Brzev et al., 2013) while a few
192 more are of national or regional reference (e.g., ATC, 1985; Grünthal, 1998) although they might have been
193 applied to wider contexts. The structural characteristics used in early classification systems such as ATC-13
194 (ATC, 1985) or European Macroseismic Scale (EMS '98) (Grünthal, 1998) were limited to the identification
195 of the main loadbearing system, and the corresponding building typologies are very generic. More recent
196 classifications systems include improved technical understanding of the parameters that more accurately
197 define the seismic response, such as diaphragm flexibility, structural irregularities, openings, behaviour of
198 non-structural components, etc. The U.S. Geological Survey (USGS)'s Prompt Assessment of Global
199 Earthquakes for Response (PAGER) program developed a global construction type catalogue (Jaiswal and
200 Wald, 2008; Jaiswal et al. 2011) based on the analysis of databases from different countries across the world.
201 It captures most of the key structural aspects that affect the seismic performance (i.e., material and type of
202 load-bearing structure, lateral resisting system, diaphragm type and height of the structure) in its primary
203 classification. It has been used widely in different regions across the world, to forecast the level of damage in
204 the immediate aftermath of main shocks. This classification system does not explicitly rank the typology
205 parameters in terms of their influence on the seismic performance. On the other hand, the Global Earthquake
206 Model (GEM) global taxonomy system (Brzev et al., 2013) is based on the concept of ordering the
207 parameters determining the response from more generic to more specific, so that for each additional
208 parameter considered, the resulting class is a subset of the one determined without that parameter. The
209 system has two main categories: primary parameters describing general building characteristics (e.g. height)
210 and secondary parameters (e.g. height above grade, story height etc.) describing the characteristics in more
211 detail. This classification system is more comprehensive than the previous classifications and results in a
212 unique taxonomy string to each building structure.

213 Rapid Visual Screening (RVS) procedures are complementary to classification system and are necessary to
214 identify, inventory, and screen buildings that are potentially vulnerable to natural hazards according to a
215 predetermined classification system. RVS procedures typically consists of methods and forms that allow
216 users to collect a modest number of parameters from a given observed building, to quickly rate its physical
217 vulnerability and rank it with respect to given benchmark or relatively to other buildings. RVS are usually
218 only the first step in seismic assessment study, whereby buildings falling short of a given benchmark, are
219 further assessed using appropriate structural analysis to determine its deficiencies and, if necessary, to
220 recommend retrofitting/strengthening interventions or replacement. An early reference is the first edition of
221 FEMA P-154 (FEMA, 1988), providing a procedure to evaluate the seismic safety of large buildings'
222 inventories quickly and inexpensively (with minimum access to the considered buildings), to screen the ones
223 requiring a more detailed examination. In 2014, FEMA automated the paper-based screening procedure of
224 FEMA P-154 by producing a mobile application (ROVER - Rapid Observation of Vulnerability and
225 Estimation of Risk), enabling users to document and transmit data gathered in the field.

226 In the past two decades, similar rapid surveying procedures have been proposed by different authorities and
227 organization, such as the World Health Organization (WHO) and the United Nations (UN), with some
228 studies focusing on assessing public buildings in developing countries (e.g., Nepal and Kyrgyzstan),
229 including schools.

230 Dhungel et al. (2012) collected and assessed the physical condition of 1,381 building units from 580 schools
231 in Nepal. The data was collected by mobilizing the school teachers; school vulnerability was used to estimate
232 the possible damage/casualties/injuries for earthquakes of different intensities. A study conducted by Grant
233 et al., (2007), proposed a multiple-level procedure aiming to identify the highest-risk buildings based on
234 filters of increasing detail, and reduces the size of the building inventory at each step. This produced a
235 prioritization scheme for seismic interventions in school buildings in Italy. With respect to other natural
236 hazards, Pazzi et al. (2016) assessed the safety of ten schools in Tuscany, Italy, against geo-hydrological
237 hazards (i.e., seismic, slope instabilities, floods and excessive surface runoff) using an RVS method. The
238 study proposes a geohazard safety classification (GSC) of schools and provides useful information to local
239 decision-makers. The GSC is calculated integrating data by means of rapid and not invasive field surveys
240 and questionnaires distributed to the school's employees.

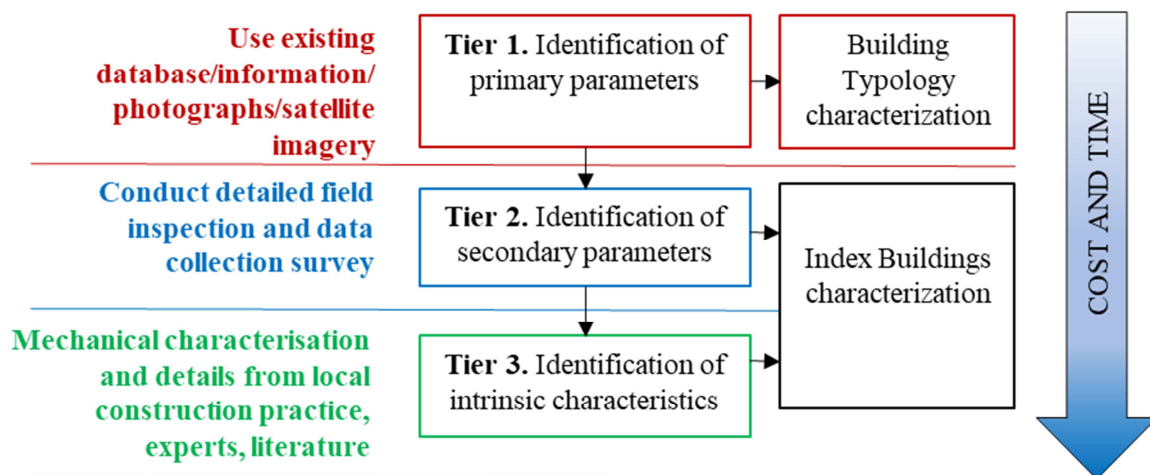
241 The above classification systems are either primarily focused on residential buildings or they consider very
242 specific local school typologies, therefore are of limited applicability because school buildings in many cases
243 have different construction/architectural characteristics (e.g., large classroom size, large and many openings,
244 etc.) than that of residential buildings and local school buildings typologies cannot be precisely categorized
245 using existing classification systems. Thus, a comprehensive building taxonomy specific to school buildings
246 for seismic vulnerability and risk assessment has been developed within the GPSS framework.

247

248 **2.2. The GLOSI classification system**

249 The GLOSI classification system was initially developed for school masonry structures, using national scale
250 case studies available to the World Bank's GPSS program, specifically the SIDA study (Adhikari et al.,
251 2016) conducted for Nepal after the Gorkha 2015 earthquake, the MARN study for El Salvador (MARN
252 2012) and the work by Yamin et al. (2015) for school infrastructure in Peru. These three databases varied
253 greatly in terms of geographical extent, attributes, number of data entry and building typologies, reflecting
254 different construction practices, and different initial motivations for their collection. To construct a taxonomy
255 of global validity, the structure and content of these databases were compared to the GEM taxonomy
256 structure (Brezv et al. 2014) and the PAGER classification (Jaiswal et al., 2011) to identify and rank
257 parameters essential to characterize the building seismic performance. These parameters are categorized into
258 primary parameters, secondary parameters and intrinsic parameters, as depicted in Figure 1, each level and
259 set becoming essential to conduct different operations in the build-up of the fragility and vulnerability
260 functions library. The identification of the primary parameters, relatively simple and mainly accomplished by
261 desktop studies of existing databases and photographic records, leads to the identification of large classes of
262 school buildings typologies, which allow inventory at national or regional level. This first activity is
263 relatively inexpensive and should be conducted by the education authority in each country to simply classify
264 their assets. The correct identification of the secondary parameters and their attributes requires field survey,
265 knowledge of national/local construction practices and regulations and a fair amount of technical expertise.
266 The classification of secondary parameters leads to the determination of *index buildings*, individual

267 structures representative of specific structural typologies whose seismic behaviour is fully identified in
 268 qualitative terms by this set of parameters and distinguishable from other structures. Finally, in order to
 269 conduct a full engineering assessment, to quantify fragility, several measurable parameters are needed,
 270 relating to both the architectural layout and the structural component of the building. As, in school
 271 architecture the number of typologies in any given country is usually relatively modest, and schools are often
 272 built according to national guidelines and models, some of this information can be obtained from blueprints,
 273 while other need to be measured on site, but it can be limited to few typical buildings. Time and cost of data
 274 acquisition increases substantially from tier 1 to tier 3 parameters, as shown in Figure 1, hence the
 275 identification of index buildings, of applicability beyond national boundaries, for which fragility and
 276 vulnerability can be ascertained with acceptable levels of confidence, is essential to deliver seismic
 277 vulnerability assessment at cost and global scale. The application to the case study in the Philippines with the
 278 development of a rapid survey smartphone-based app, presented in section 3 of this paper, shows how this
 279 part of the procedure can be expedite in practice and generalized also to other hazards.



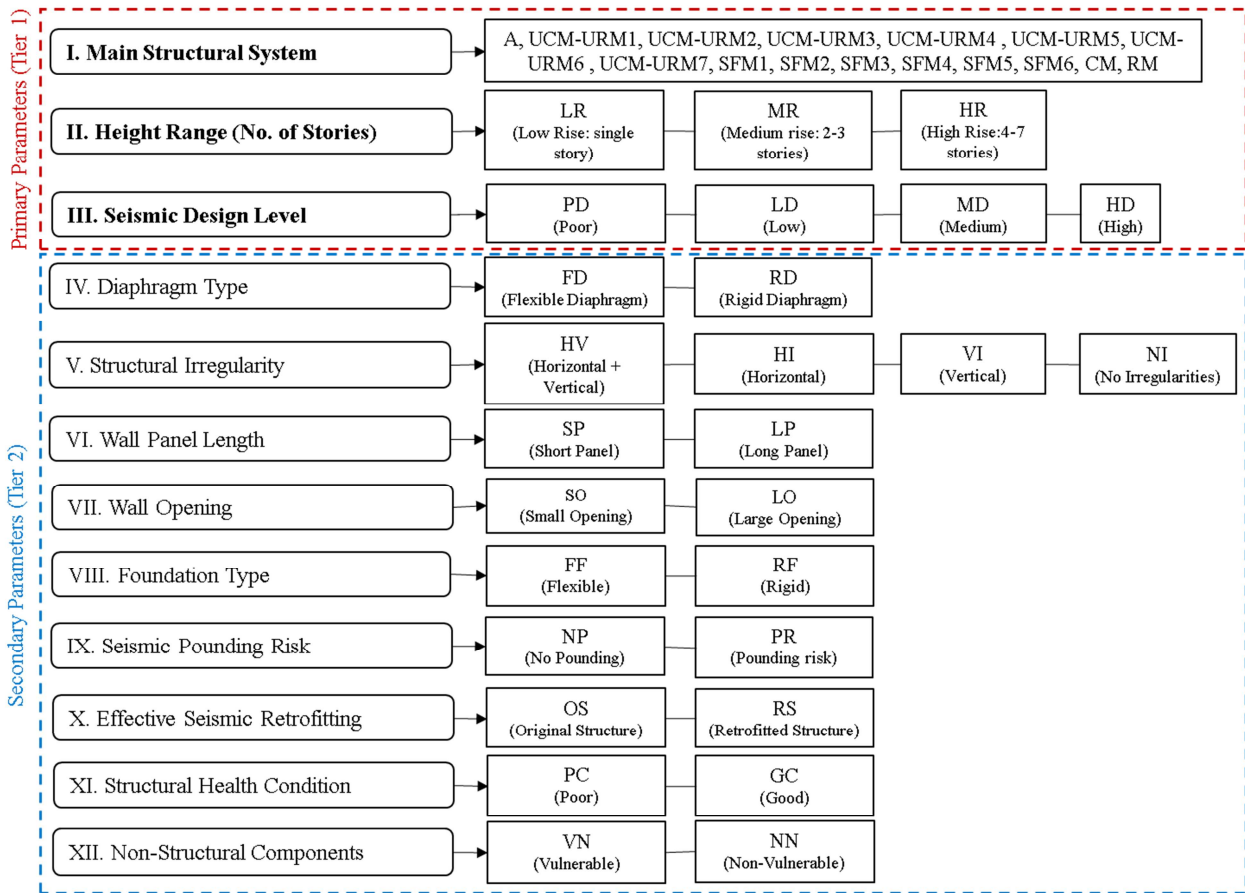
280

281 **Figure 1. GLOSI Classification system: Layers of refinement and need for resources in building data acquisition**
 282 **(The World Bank, 2019)**


283 The specific parameters considered in the GLOSI taxonomy system and their attributes are summarized in
 284 Figure 2, for masonry structures. More discussions on the different vulnerability parameters and their
 285 attributes can be found and Adhikari et al. (2018). Tier 1 includes the load bearing system, the height range
 286 and the seismic design level. The attributes associated with these parameters collectively define a building
 287 type. The main structural system defines fundamental aspects of the expected seismic behaviour such as the
 288 response to horizontal loads, the lateral strength of the building and its ductility. For unreinforced masonry
 289 structures, just by considering the nature of unit and mortar components, 8 basic typologies are identified,
 290 from adobe to roughly squared stone solid masonry in mud mortar, for instance. Considering also masonry
 291 combined with light steel frame and reinforced and confined masonry, leads to a total of 16 basic masonry
 292 typologies. For each of these, the height of the building is a second important parameter which controls the
 293 vibrational characteristics of a building structure. The seismic design level provide insight to the extent to
 294 which the building is designed to resist seismic actions. If the building is engineered the seismic design level
 295 will represent the set of recommendation included in the seismic code of the location at the time of
 296 construction of the building. However, in countries such as Nepal or Perú, it is common that school buildings
 297 be mostly constructed by local communities without adherence to seismic codes or guidelines, even when in
 298 force (Dixit et al., 2014; Yamin et al., 2015). Thus, several factors such as the designer and contractor (e.g.
 299 government, community, private contractor etc.), local code enforcement capacity, workmanship and level of
 300 quality control during construction influence the seismic design level and should be assessed prior to assign a
 301 design level class to a specific building. Notion of the seismic building culture of the country and its
 302 evolution is essential. These three parameters allow to determine broad typologies of buildings such as
 303 “unreinforced brick masonry in cement mortar, 1 storey high, with good connection of orthogonal walls,
 304 corresponding to medium design level”. The total number of possible combinations for masonry structures
 305 when only the primary parameters are considered is equal to 192. These are clearly applicable worldwide
 306 and easily identifiable through educational authority documents.

307 The secondary parameters are a group of characteristics that play a key role in modifying the expected
 308 behaviour of a building as identified by tier 1 parameters (see Figure 2). For each of these parameters, using


309 the evidence from available databases, a set of attributes is identified, which characterize the seismic
 310 response. While the Tier 1 parameters are common to other classification systems, the secondary parameters
 311 and their value range are chosen specifically to represent the construction characteristics typical of school
 312 architecture, affecting their seismic response, such as wall panel and opening size and layout.



313 **Figure 2. Vulnerability parameters and attributes of tier 1 and tier 2 component of the GLOSI taxonomy system**
 314 **(The World Bank, 2019).**
 315



Front View



Side View

A brick in mud mortar school building in Nepal (Photo credit: The World Bank)

Main Structural System - UCM-URM4
Height Range - LR(1)
Seismic Design Level - PD
Diaphragm Type - FD
Structural Irregularity - NI
Wall Panel Length - LP
Wall Opening - LO
Foundation Type - RF
Seismic Pounding Risk - NP
Effective Seismic Retrofitting - OS
Structural Health Condition - PC
Non-Structural Components - VN

GLOSI Taxonomy String

UCM-URM4/LR(1)/PD/FD/NI/LP/LO/RF/NP/OS/PC/VN

317 **Figure 3. Vulnerability attributes and taxonomy string for a single storey load bearing masonry school building.**
 318 **Note that the primary parameters are given in boldface. (The World Bank, 2019)**
 319
 320

321 According to this system, the scoring of this secondary parameters determines the index buildings specific of
322 a regional or national study (Figure 3). This can be achieved by a mixture of analysis of documentation and
323 limited site surveys. Each index building is then uniquely identified by a 12-parameter string, providing a
324 sort of DNA classification, which allows to group together buildings from different regions but with similar
325 construction and structural features and expected to have same seismic performance. Once the classification
326 system is developed, strings can be generated for each combination of the attributes of the 12 parameters and
327 this would result in a diverse population in excess of 196000 index buildings, all in theory possible, for
328 which fragility and vulnerability could be analytically computed, provided tier 3 parameters are also
329 available. Such computational effort would then provide a complete repository of fragility and vulnerability
330 functions for load bearing masonry structures fully accessible and applicable worldwide. Hence at the local
331 level, once a building is surveyed, then it is sufficient to match the resulting taxonomy string with the correct
332 identifier in the repository, to obtain fragility and vulnerability for that particular index building. In fact, not
333 all combinations are realized in practice, especially for what concern the Tier 2 parameters, as they are
334 indicative of structural quality and usually there is some consistency among them. These substantially
335 reduces the number of realistic taxonomy strings to a few more than 1500 masonry index buildings. Still a
336 large number, but one that the global engineering community can deliver with relatively modest resources.
337 Moreover, when assessing a specific index building in the field, not all the information required might be
338 known. This means that the completeness of the taxonomy string depends on the extent of information on the
339 building characteristics; when limited information is available, any element in the string can be omitted or
340 truncated depending on the availability of the information or priorities given to different taxonomy
341 parameters. In such situations, the matching with the original index buildings string will be partial and more
342 than one fragility functions might be appropriate, in the first instance. This however will lead to increased
343 uncertainty in respect to the actual vulnerability of the structure. Within the GLOSI programme, a specific
344 task conducted is a sensitivity analysis to ascertain the relevance of any of the tier 2 parameters (The World
345 Bank, 2019).

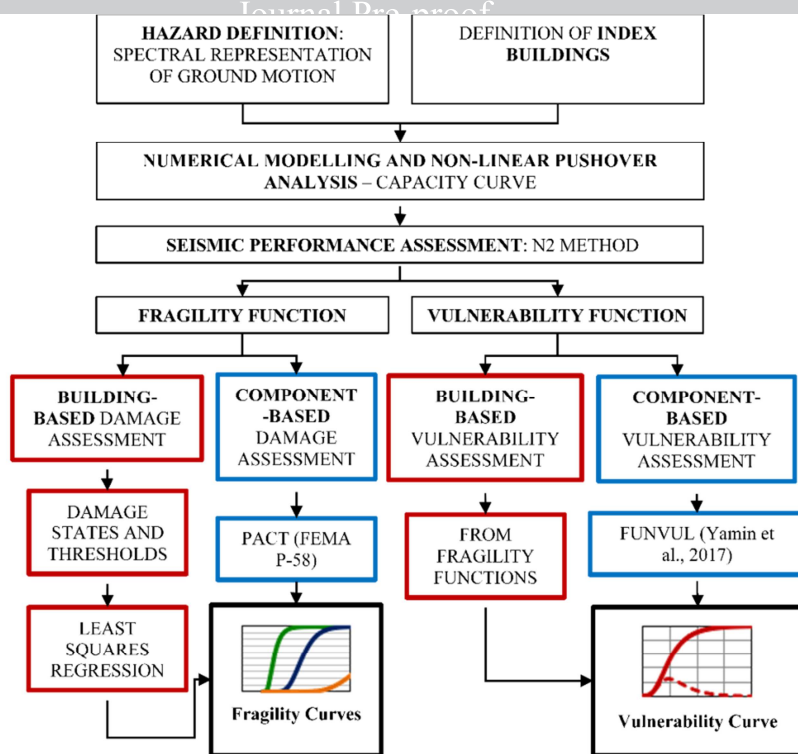
346

347 **2.3. From index buildings to analytical fragility-based vulnerability**

348 The intrinsic parameters, forming tier 3 of the GLOSI building data system, are the building-specific
349 characteristics such as the geometric dimensions, architectural layout and the mechanical properties of the
350 construction materials/structural elements. Even though these are not explicitly included in the taxonomy
351 string, these parameters are required for the complete definition of index buildings and for the development
352 of reliable analytical models, which constitute the basis on which fragility and vulnerability functions are
353 computed. A wide range of methodologies are available in the literature for the seismic fragility and
354 vulnerability assessment of representative buildings (D'Ayala et al, 2015, Yamin et al., 2017). Approaches
355 may consider empirical or expert opinion-based or analytical or hybrid methods for the derivation of fragility
356 and vulnerability functions. For the GLOSI library, the analytical vulnerability approach is adopted, as it
357 allows for an unbiased and consistent assessment applicable worldwide, independently of historic seismic
358 damage data and local expertise on specific typological building performance (Rossetto et al., 2014). The
359 general methodological approach proposed in the framework of GLOSI to generate representative and
360 comprehensive fragility and vulnerability functions for an index building can be summarized in the
361 following steps, reproduced in Figure 4:

- 362 • The seismic hazard is defined in terms of the acceleration spectra. Natural earthquake records can be
363 implemented as demand to generate unsmoothed spectra as opposed to the conventional capacity
364 spectrum method, which utilizes standardized design spectra. Therefore, the resultant performance
365 points will account for the natural variability of the seismic demand. However, the outcomes are highly
366 sensitive to the chosen ground motion records. For the GLOSI, the far-field ground motion set
367 suggested in FEMA P-695 (FEMA, 2009) has been applied. The set of records are designed to be
368 neither structure- nor site-specific and consists of 22 record pairs, hence particularly suited to the
369 GLOSI application to a wide range of structures worldwide. Each pair consist of two horizontal
370 components for a total of 44 ground motions. The records have a moment magnitude (M) range of 6.5 to
371 7.6 with an average magnitude of 7.0 and all were recorded at sites located at a distance greater than or
372 equal to 10 km from the fault rupture. According to the soil classification of NEHRP (FEMA-450,
373 2004), 16 sites are classified as stiff soil site (type D) and the remaining are classified as very dense soil
374 (type C), also providing variability in the natural site response amplification.

- 375
- 376
- 377
- 378
- 379
- 380
- 381
- 382
- 383
- 384
- 385
- 386
- 387
- 388
- 389
- 390
- 391
- 392
- 393
- 394
- 395
- 396
- 397
- 398
- 399
- 400
- 401
- 402
- 403
- 404
- 405
- 406
- 407
- 408
- 409
- The index buildings computational models are defined as explained in the previous section by using the taxonomy parameters and intrinsic characteristics (geometrical characteristics and material properties), determined at different sites. Their seismic capacity is computed by performing static equivalent pushover analysis. This provides a good reference level, which professionals in many countries can achieve and control with confidence, if they want to develop consistent fragility functions for inclusion in the GLOSI. For each index building, 3-D numerical models are generated, and non-linear pushover analyses are performed to generate capacity curves. A wealth of different methodologies is available in literature and corresponding software commercially available can be used for the pushover curve derivation. It should be noted that for Load Bearing Masonry structures with flexible diaphragm, the pushover curves are generated with respect to global in-plane and global out-of-plane behaviours separately. The reasons for this approach are discussed in detail in Adhikari and D'Ayala (2019).
 - The seismic performance assessment is carried out using the latest version of the N2 method (Fajfar, 2000, D'Ayala et al., 2015). For each pushover curve, the thresholds of discretized damage states represented by the roof drift are determined in terms of specific element damage and global damage indicators. The definition of damage states and associated threshold limits can be code-based, from the available literature or index building specific. In GLOSI, the approach adopted is to identify index building - specific damage states, obtained through validation with experimental and field observations available in literature. This is preferred to the reliance on code prescriptions, sometimes derived through expert opinion, and not easily traceable. For each IB, the MDoF pushover curves are converted to bilinear idealized pushover curves of the equivalent single degree of freedom system (SDoF) following standard rules. This is then intersected to the demand spectrum of each of the different ground motions pairs (scaled to different values of IM) to generate a number of performance points (IM vs. EDP) within each damage class, sufficient to perform regression analysis.
 - The derivation of fragility functions is conducted at building scale, rather than component scale, for each damage state. The least square regression method is used for each damage state (D'Ayala, 2015). It should be noted that for flexible diaphragm type LBM structures, the fragility curves are generated with respect to global IP and global out of plane (OOP) behaviours separately (Adhikari & D'Ayala, 2019).
 - Finally, for the derivation of vulnerability functions, for the load bearing masonry index buildings, the computation is first performed for each set of walls depending on the damaging regime (in-plane or out-of-plane) convolving the fragility curve with a uniform cost function, and then the cumulative vulnerability is computed, to reflect the different levels of damage of different components for different values of the intensity measures.
 - On the other hand, in the component-based fragility/vulnerability assessment, component (e.g. each column, beam-column joint, infill wall etc.) level fragility curves (FEMA P-58) are used to arrive at the vulnerability function. Detailed procedure is given in Yamin et al. (2017).



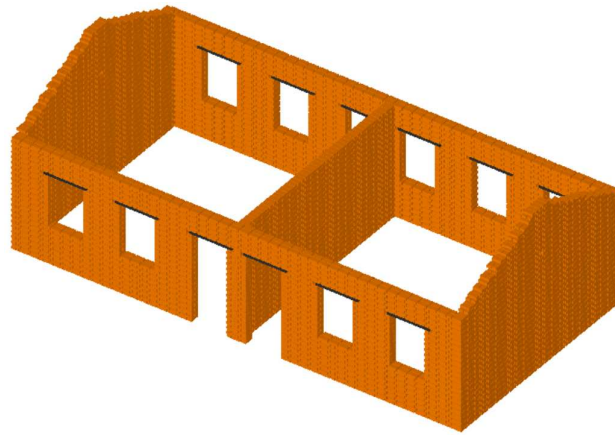
411
412 **Figure 4. GLOSI fragility and vulnerability assessment methodology. Note that the red and blue colours**
413 **represent steps for building-based and component-based fragility/vulnerability assessment methodology,**
414 **respectively. (The World Bank, 2019)**
415



416
417 **Figure 5. Photographs representative of an IB of the UCM-URM7/LR(1)/LD school building type: (left) outside**
418 **front view and (right) Inside view showing the flexible roof diaphragm. (Photo from Nepal, Copyright: The**
419 **World Bank).**

420 The corresponding taxonomy string for this index building is **UCM-URM7/LR(1)/LD-**
421 **/FD/Ni/LP/LO/RF/NP/OS/PC/VN**, where the Tier 2 parameters refer to flexible diaphragm (FD), no
422 irregularities (Ni), long panels (LP) meaning that the length of wall transversally unrestrained is larger than
423 12 time the wall thickness, large opening (LO) meaning that the void to mass ratio in the longitudinal walls
424 is higher than 50%, rigid foundation (RF), meaning that it is built on a thick strip foundation, no pounding
425 risk (NP) as it is isolated, no retrofitting or strengthening (OS, original structure), poor maintenance
426 condition (PC), and presence of vulnerable non-structural elements (VN). Figure 6 shows the element by
427 element 3-dimensional numerical model developed in Extreme Loading for Structures® (ELS) software
428 (ASI, 2018) using the applied element method. Average material properties for the UCM-URM7
429 construction in Nepal were obtained from Guragain (2015). A global pushover analysis is conducted in 3-D
430 numerical model in the two orthogonal directions, transversal and longitudinal, by increasing linearly the
431 base acceleration with time until the building reaches collapse. The pushover curves are obtained by
432 computing the base shear in each set of walls and the corresponding displacement of a control point on the

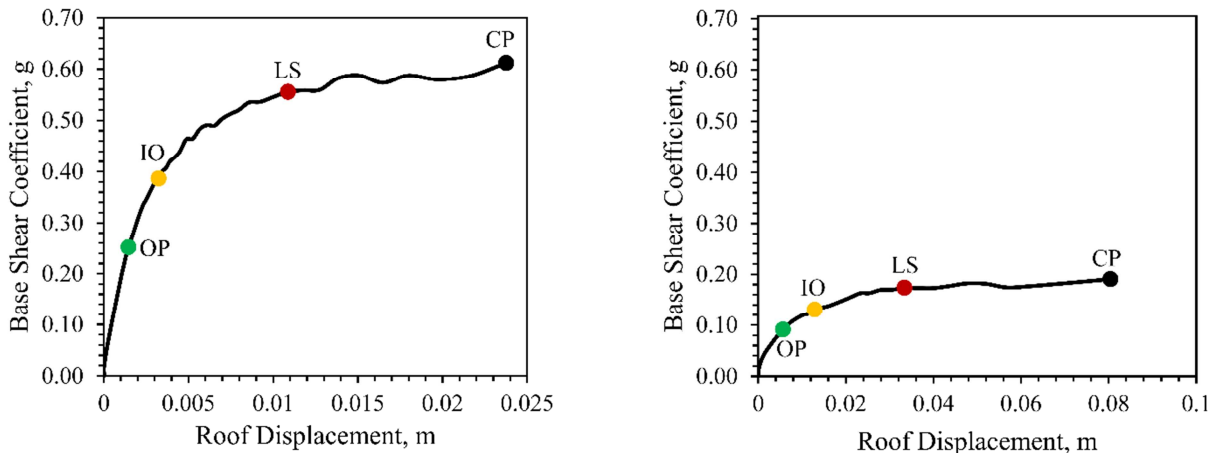
433 same wall. As the longitudinal direction results to be the weakest, the consequent fragility and vulnerability
 434 analysis is conducted in the longitudinal direction only.



435
 436 **Figure 6. Numerical model of the UCM-URM7 IB in ELS using simplified micro-modelling technique.**

437 Figure 7 presents the global capacity curves with respect to in-plane (IP) and out-of-plane (OOP) behaviour
 438 respectively. The capacity of the OOP walls is governed by its low overturning capacity heightened by the
 439 poor quality of cross wall connections (i.e. insufficient interlocking of bricks at corners, leading to low
 440 friction capacity). Four performance level thresholds are also identified on each curve, corresponding to the
 441 Operational, Immediate Occupancy, Life Safety and Collapse Prevention performance criteria (as defined in
 442 Table 1). The position of these thresholds on a given capacity curve is identified in relation to the
 443 development of the crack pattern and maximum roof drift achieved by the two sets of orthogonal walls
 444 independently, as the stiffness and strength of each sets of walls is substantially different.

445



446

447 **Figure 7. Capacity curves and associated performance level thresholds for the UCM-URM7 IB: global IP**
 448 **behaviour (left) and global OOP behaviour (right). (Performance level thresholds: green – Operational, yellow –**
 449 **Immediate Occupancy, red – Life Safety and black – Collapse Prevention).**

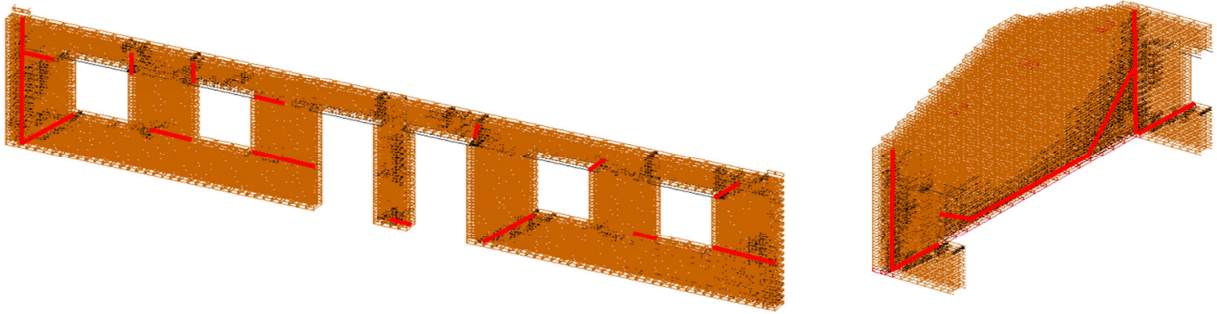
450

451 **Table 1. Example physical definition of performance level thresholds for an unreinforced masonry wall under IP**
 452 **behaviour.**

Performance level threshold	Physical damage definition
Operational Threshold (OP)	Hairline cracks (about 0.1 - 1 mm width) on few corners around the openings.
Immediate Occupancy Threshold (IO)	Hairline to minor cracks appear on all the corners around opening, minor tensile cracks of about 1 mm - 5 mm width appeared in few spandrels, diagonal shear cracks (about 1 mm - 5 mm maximum width) start to appear in some piers.

Life Safety Threshold (LS)	Most of the piers and spandrels have developed minor tensile/diagonal shear cracks (about 5 mm in width). Few spandrels and piers start to develop major flexural/shear cracks of 10 mm maximum width.
Collapse Prevention Threshold (CP)	Most of the spandrels and piers have already developed a major crack of about 10 mm width. Few spandrels damaged with an extensive crack width of 10 mm to 15 mm and few piers start to develop extensive cracks in shear or combined shear-flexure mechanism with a maximum crack width of about 15 mm.

453



454

455

456

Figure 8. Damage distribution at collapse for the two sets of walls (left – IP wall, right – OOP wall) of the UCM-URM7 index building. Red lines highlight the failure mechanism.

457

458

459

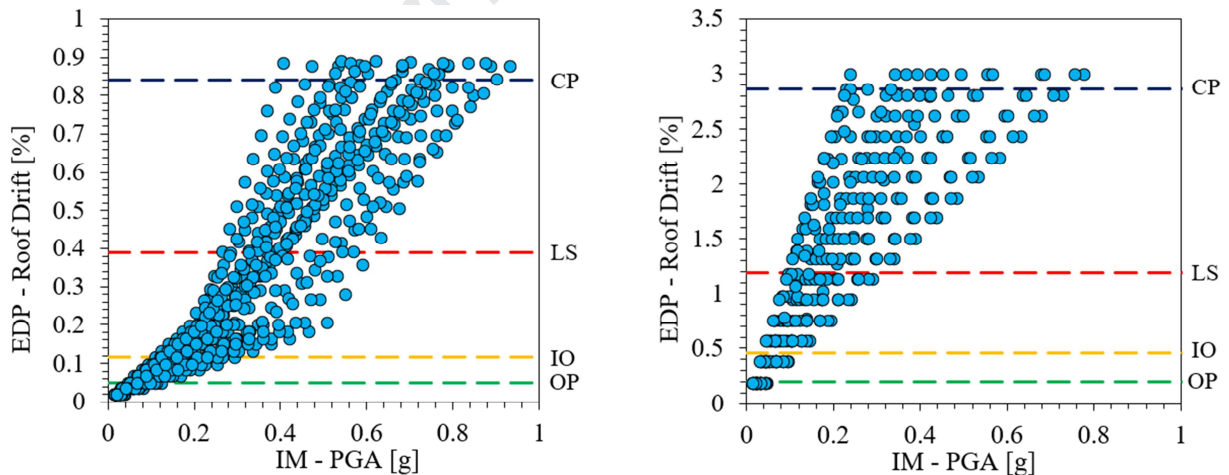
460

461

462

To perform the fragility analysis, using the N2 method, the capacity curves are reduced to equivalent SDOF bilinear curves and a performance point cloud (IM vs EDP) is obtained separately for the IP and OOP behaviour using the set of 22 ground motions pairs (each scaled at increments of 0.05 g between PGAs of 0.00 and 1.00 g). The substantially different shape and range of the two point-clouds shown in Figure 9 further proves the legitimacy of assessing the two sets of walls independently.

463



464

465

466

Figure 9. Performance points (IM vs EDP) for IP behaviour (left) and OOP behaviour (right) for the UCM-URM7 index building. Coloured lines represent the threshold of different performance levels.

467

468

469

470

471

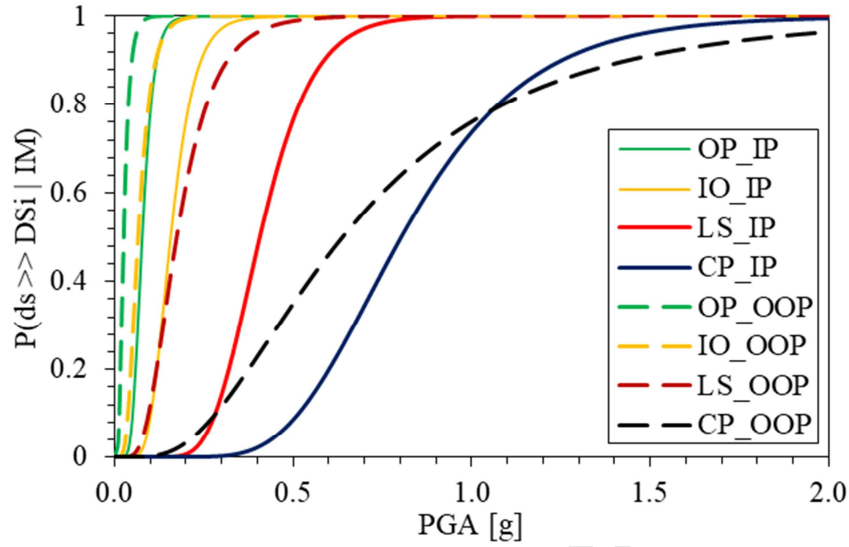
472

473

474

To derive the fragility functions from the IM-EDPs performance points generated with the N2 method, a least square regression is used, bracketing the performance points bin in each damage state range. A PGA of 2g is considered as the upper limit of the IM. Usually the value of the spectral acceleration corresponding to the natural frequency of the structure or substructure, $S_a(T)$, is considered as a more meaningful IM to express fragility, as it is a measure of the specific acceleration exerted on the structure or its parts, depending on their stiffness and strength (see section 3). However, in this case, as the IP and OOP walls are part of the same structure, but experience very different $S_a(T)$, a common reference is needed, and hence the peak

475 ground acceleration (PGA) is more appropriate. Indeed, the visual comparison of the fragility curves
 476 immediately conveys the lower fragility of the in-plane walls up to the limit state of life safety. However for
 477 the collapse prevention limit state, given the limited ductility of the in-plane walls with respect to the out-of-
 478 plane walls, the probability of collapse is slightly smaller for the latter for $PGA > 1.0g$ (Figure 10).



479
 480 **Figure 10. Fragility curves for different performance levels (OP – Operational, IO – Immediate Occupancy, LS –**
 481 **Life Safety and CP – Collapse Prevention) for UCM-URM7 index building with respect to global IP and global**
 482 **OOP behaviour.**

483
 484 Finally, for the generation of building-based vulnerability curves, the procedure suggested in D’Ayala et al
 485 (2015) is employed. The probability of a building sustaining a particular damage state requires the
 486 calculation of damage probabilities from the fragility curves for specific intensity levels. This is
 487 accomplished by calculating the difference in probability of exceedance between successive curves, for each
 488 given value of interest of the intensity measure. For the situation depicted in Figure 10, where four damage
 489 states (i.e. performance levels) are considered, the computation of corresponding mean and variance of the
 490 vulnerability function are given as:

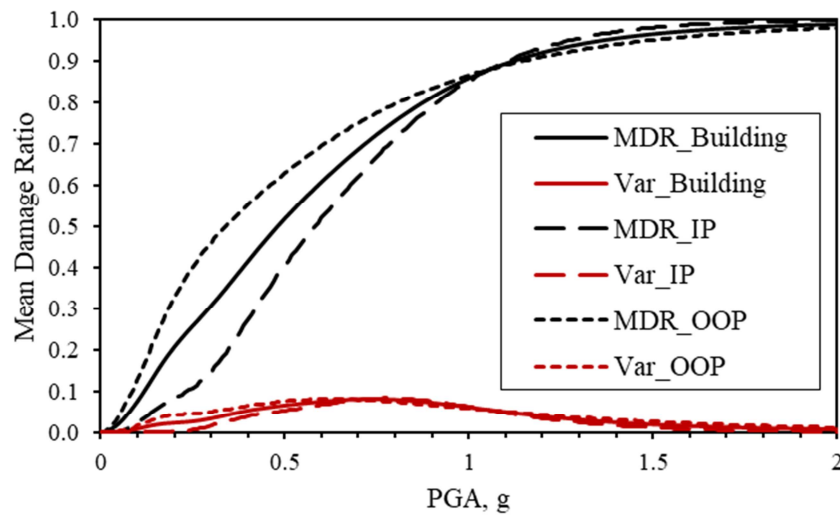
$$491 \quad E(C|im) = \sum_{i=1}^n E(C|ds_i) \cdot P(ds_i|im) \quad (1)$$

$$492 \quad var(C|im) = \sum_{i=1}^n [E(C|ds_i) - E(C|im)]^2 \cdot P(ds_i|im) \quad (2)$$

493 where, $E(C|im)$ is the mean of the vulnerability function (cost or loss) given an im ; n ($= 4$) is the number of
 494 damage states considered; $P(ds_i|im)$ is the probability of the structure sustaining a damage state ds_i given
 495 an intensity level im ; $E(C|ds_i)$ is the mean value of the cost (or loss) given ds_i ; and $var(C|im)$ is the
 496 variance of the cost (or loss) given an im .

497 Repeating the application of equations (1) and (2) for different values of im will result in the vulnerability
 498 curve and their variance depicted in Figure 11.

499 Figure 11 shows the vulnerability functions with respect to global IP and global OOP behaviour. The same
 500 also presents the building total vulnerability curve obtained by combining these two vulnerability curves by
 501 using the proportion of mass of walls under IP behaviour and walls under OOP behaviour (50% each in this
 502 case).



503
504 **Figure 11. Vulnerability curves and variance with respect to a) IP behaviour (MDR_IP), b) OOP behaviour**
505 **(MDR_OOP), and (c) building total vulnerability curve (MDR_Building) for the UCM-URM7 index building.**

506

507 The derivation of vulnerability functions in terms of mean damage ratio allows the comparison of expected
508 losses between very different types of index- school buildings, given equivalent expected seismic hazard.
509 The variance curves included in Figure 11 allows to understand the level of confidence associated with this
510 type of evaluation. This also can vary from index building to index building. Further uncertainties in the
511 vulnerability functions are associated with respect to the reliability of the data collection, material
512 characterization, modelling tools and methodology, capacity assessment etc., and the real variance of
513 building response, even for the same index building, due to variation in materials and construction on site.
514 Hence it should be understood that the vulnerability curves shown in Figure 11 are mean values only, while
515 the variance shown may appear not so significant for the reason that not all the elements of uncertainties are
516 considered herein.

517 Such vulnerability functions are an essential ingredient of seismic risk assessment at regional and country
518 levels. In order to progress from vulnerability to risk assessment, the functions produced with the GLOSI
519 procedure expounded above need to be convolved with scenarios of the spatial distribution of the hazard in
520 terms of expected value of the chosen intensity measure at each point, given a return period, and of the
521 distribution of each index school building (exposure) over the territory, for a given region or nation. Hence
522 the global vulnerability functions developed within GLOSI provide a common benchmark to compare
523 parametric risk mitigation programmes, for different countries or regions, based on a common multi-criteria
524 approach.

525 A complete risk mitigation programme at national level requires the assessment of the vulnerability of the
526 whole school building assets' portfolio, the hazards they are exposed to and the effectiveness and viability of
527 different strengthening strategies. Risk mitigation can also be achieved by implementing simple set of
528 actions, relevant to the use of the buildings, which can have a substantial effect in reducing the vulnerability
529 of the occupants. In the following section, some of these activities, as developed through two collaborative
530 projects sponsored by the UK and the Philippines research councils are presented with reference to primary
531 school buildings in the city of Cagayan de Oro. This allows to focus the discussion on a real case study,
532 understand the burden and possible solutions for data acquisition, show how some of the approaches and
533 methodologies discussed in this section can be expanded with reference to other hazards, highlight how the
534 effectiveness of strengthening strategies can be accounted for and used to support risk mitigation
535 programmes.

536

537

538 **3. The experience of the Philippines: multi-hazard physical vulnerability prioritization of schools and**
539 **retrofitting strategies.**

540 According to the *Index for Risk Management 2020* (INFORM, 2019), the Philippines, with a population of
541 108.12 million, ranks 3rd in terms of natural hazards among countries most exposed to multiple hazards, with
542 a high score of 8.5 out of 10.

543 Located in the Pacific Ring of Fire, the country is highly exposed to earthquakes, volcanic eruptions, and
544 other geological hazards, as well as to multiple typhoons and monsoon rains. An average of six tropical
545 cyclones make landfall in the Philippines annually with another three-passing close enough to cause loss.
546 Super typhoon landfalls occur, on average, twice every three years. Most of these occur along the relatively
547 unpopulated eastern coast; however, recent records show that the path of such typhoons is moving westward
548 and northward (Takagi and Esteban, 2016). Because of weak steering currents, storms tend to move slowly
549 across the Philippines. As a result, heavy precipitation is very common and thus flood risk is generally high
550 across the country. For instance, it is not uncommon for more than 500 mm of precipitation to fall across a
551 large area, with more than 1,000 mm having been observed across the mountains of Luzon (Racoma et al.,
552 2016).

553 Due to the mentioned hazards, combined with high level of poverty, various communities throughout the
554 Philippines are left in highly-vulnerable situations. In recognition of the country's vulnerability to natural
555 hazards, the enactment of the Philippine Disaster Risk Reduction and Management (DRRM) Act in 2010
556 (Republic Act No. 10121) enabled substantial progress in shifting the emphasis from emergency response to
557 preparedness, mitigation and prevention. Significant resources have been provided for ex-ante investments
558 and new areas of engagement have been considered in the policy dialogue. However, challenges remain
559 (e.g., limited financial resources, limited technical skills and tools) in enabling implementation of disaster
560 risk reduction investments in priority sectors, including education.

561 Taking advantage of the opportunities for international collaboration through the UK Engineering and
562 Physical Sciences Research Council (EPSRC) Global Challenges Research Fund (GCRF) and the British
563 Council Newton Fund, the authors have initiated a three-year long partnership with colleagues from De La
564 Salle University in Manila and Xavier University in Cagayan the Oro, working on vulnerability assessment
565 and resilience of school infrastructure to multi-hazard in the Philippines. Within this framework, the
566 partnership has developed several tools: a rapid visual screening (RVS)-based multi-hazard vulnerability
567 prioritization procedure for asset ranking; a detail procedure for empirical vulnerability assessment of school
568 compounds to flooding; an analytical seismic vulnerability assessment and retrofitting framework; a
569 multicriteria procedure to determine the suitability of school infrastructure as evacuation and population
570 shelter centres; a large volume of material for training and knowledge exchange available on line. The
571 present paper focus on some of these outputs which best illustrate the methodology introduced in the
572 previous section.

573 Specifically, the next section discusses the RVS procedure for multi-hazard vulnerability prioritization and
574 its implementation in a mobile application to efficiently assist the surveyors. A physical vulnerability index
575 for each hazard is then proposed. An illustrative application of the developed tools is presented for the city of
576 Cagayan de Oro, Philippines, relating the collected data for 115 school buildings to the proposed
577 vulnerability index to swiftly determine the most vulnerable structures among the surveyed stock. The
578 overall aim is to prioritize a more detailed survey phase for identified index buildings, conduct a more
579 detailed seismic performance assessment through the analytical fragility/vulnerability approach introduced in
580 the previous section, and determine suitable strengthening strategies.

581

582 **3.1. Rapid Visual Surveying via mobile application**

583 The proposed RVS procedure for multi-hazard vulnerability prioritization uses a sidewalk survey of school
584 building, aided by a data collection form, which the surveyor can complete, based on visual observation of
585 the building from the exterior (and if possible, the interior), without requiring detailed structural drawings or
586 calculation reports. The one-page data collection form, shown in Figure A-1, is based on decade-long
587 expertise of the authors on this type of surveys for diverse hazards (e.g., D'Ayala & Speranza 2002, D'Ayala
588 & Paganoni 2011, Stephenson & D'Ayala 2014) and adopts, where relevant, the GEM Building Taxonomy
589 (Brzev et al., 2014), as already discussed in section 2.2. To take into account the vulnerability to diverse
590 hazards, the geolocation of the building in relation to coasts, rivers and faults (if known), is included,
591 together with hazard categories according to the local design codes. The form also considers the exposure,
592 estimated on the basis of the number of classrooms and occupants. For the vulnerability ranking, besides the
593 Tier 1 and Tier 2 parameters discussed in section 2.2, specific information is required for the relation of the

594 building to the ground, and for the roof, which determine the vulnerability to floods and wind respectively.
595 The form also allows to consider a broad range of structural materials and lateral load resisting system, so
596 that the survey can extend to almost any building type within a school infrastructure portfolio and assess
597 them on the same basis. Depending on the structural system and material, the most common deficiencies are
598 also listed. These are referred to as vulnerability factors including potential pounding effects, presence of
599 soft-story, presence of strong-beams weak-columns, geometric irregularities, etc. The confidence of the
600 surveyor in collecting each of the input data during the assessment is also recorded with a score from High to
601 Low, depending on the thoroughness of the survey.

602 The inspection time is a function of the foot-print of the surveyed building, varying between 15 to 30
603 minutes, plus the traveling time spent between buildings. In any screening programme, it is likely that some
604 aspects of the structure cannot be identified due to the architectural finishes covering them. In this case, a
605 more detailed structural assessment can be performed to correctly identify the structural type and its
606 deficiencies. Moreover, the collected data can also be used as a basis for developing detailed numerical
607 models, for instance through a simulated design procedure for selected ‘index’ buildings as discussed in
608 section 2.3 and also in Novelli et al. (2015), Verderame et al. (2010); Gentile et al., (2019). Once the data
609 collection phase is completed, depending on the considered hazard, a subset of parameters with the highest
610 contribution to the vulnerability can be identified and ranked/weighted, similar to an approach followed by
611 Stephenson & D’Ayala (2014). Some of the parameters are shared among all hazards, such as the structural
612 lateral resisting system and the dominant construction material, while some are just specific to a particular
613 hazard, as shown in Table 2. For instance, in case of strong wind, majority of the roof characteristics are
614 considered, while for the flood hazard, the percentage and dimensions of openings have much bigger effect.

615 As already explained in section 2.2. for each parameter, a range of possible attributes can be identified, while
616 a vulnerability rating (VR) is assigned to each one based on a scale of 20 to 100, divided into equal,
617 unweighted parts according to the number of attributes, with 20 indicating the lowest vulnerability and 100
618 the highest vulnerability attribute (Stephenson & D’Ayala, 2014).

619 The ranking of the attributes within each parameter considers their relative contribution to vulnerability for
620 the specific hazard. Such a ranking is mainly based on engineering judgment and, for some parameters (e.g.,
621 lateral load resisting system and its material), makes also use of an analytical calibration based on fragility
622 and vulnerability relationships (e.g., Gentile et al., 2019). For instance, in the case of material and lateral
623 load resisting system, unreinforced load bearing masonry has the highest VR score of 100, reinforced
624 masonry 70, timber frame scores 50, reinforced concrete frame with masonry infill 30 and steel frames with
625 bracings have the lowest score of 20. Furthermore, in case of seismic vulnerability, the potential for
626 pounding, the presence of short columns or presence of infills at the ground floor are either true or false and
627 a vulnerability index is allocated accordingly.

628 Among the considered parameters, the construction year of the building plays a critical role in the
629 vulnerability assessment. Buildings of recent construction are more likely to be based on some hazard-
630 informed design and feature *ad-hoc* seismic resistance details/measures. Hence, the allocated vulnerability
631 rating for recent construction years is assumed as lower compared to that of older building designed based on
632 earlier building codes (the scoring is usually obtained by mapping the year of construction of the assets and
633 the evolution of the building code in the given region). It is worth noting that even recently built buildings
634 can be community-built and hence with limited engineering input, leading possibly to a higher vulnerability
635 score than less recent but engineered buildings. Hence, while the construction year can be a proxy for the
636 most likely construction technology used, insight into the level of engineering of the construction can be
637 surmised through the “material and lateral system combination”. However, to render this evaluation more
638 explicit, a separate indicator called “design level” is included in the GLOSI vulnerability DNA taxonomy
639 (see section 2.2). In the specific case study presented here, the buildings considered have been designed and
640 constructed by the Filipino Department of Education following the seismic design code at the time of
641 design/construction. Therefore, the case-study buildings can be considered, at least in principle, all
642 engineered.

643 To achieve an accurate scoring for prioritization, the vulnerability index corresponding to each of the
644 considered natural hazards is estimated discretely. The total vulnerability index (VI) assigned to each
645 building surveyed, is the normalized, weighted average of the scoring assigned to each parameter. Further
646 details on the rating system and calculation of VI are discussed in detail in Nassirpour et al. (2017) or Gentile
647 et al., (2019).

648

649

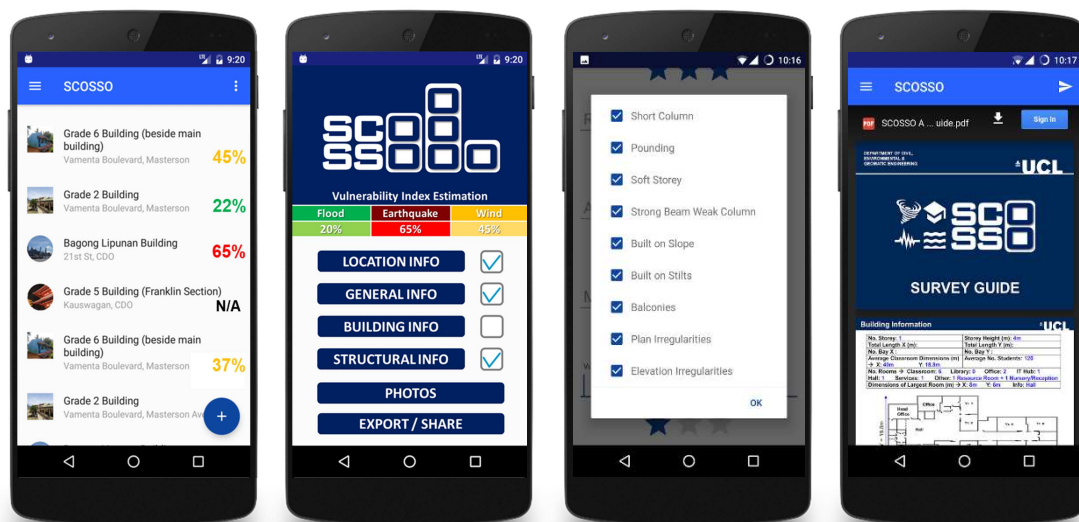
Table 2. Factors allocated for estimating the vulnerability index according to the hazard

FLOOD	EARTHQUAKE	WIND
	Material + Lateral System Combination	
	Construction Year	
	No. of Story	
	Structural Condition	
% of Opening	Floor Material	Roof Structure
	Connection Quality	Roof Covering
	Vulnerability Factors	Roof Connection
		Roof Condition
		Roof Pitch

650

651 A mobile application, the SCOSSO App (Download Link: <https://bit.ly/2YDPH7Q>), has been developed to
 652 assist the surveyors by increasing the efficiency, precision and speed of the rapid visual survey. The survey
 653 form has been implemented in the application, featuring a simple and user-friendly interface, together with
 654 an online routine to compute the vulnerability index of the building being surveyed, in real time, for different
 655 hazards, including seismic, strong wind and flood. Users can capture photos of the surveyed structures
 656 through the built-in camera tool, while the app automatically stores and allocates them to the relevant
 657 surveyed building. The survey data is stored in the mobile device as well as on the cloud and can be shared
 658 via email or extracted as a .csv file. Beside the traditional latitude and longitude location indicator, a built-in
 659 locator with a high precision of 3m by 3m squares, is also included by implementing the What3Word
 660 extension. This innovative global addressing system is becoming more common among emergency services,
 661 such as Philippine's Red Cross and United Nation's disaster relief programs. Furthermore, a comprehensive
 662 survey guide is provided, demonstrating different aspects and options of the app through visual examples,
 663 which can be used to train new surveyors. All mobile app features are fully operational offline and without
 664 any network or cellular connectivity. The SCOSSO mobile application is freely available through the Google
 665 Play Store (Figure 12).

666



667

668

669

670

Figure 12. Interfaces of SCOSSO Mobile Application

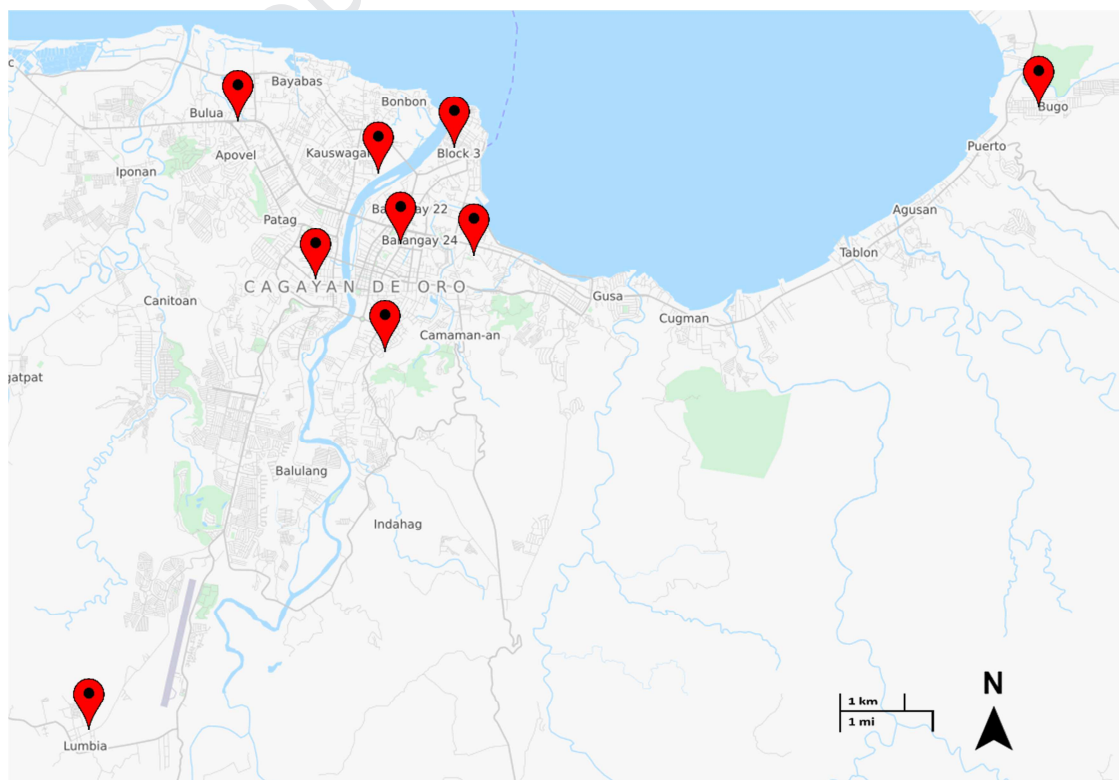
3.2. Application case study in Cagayan the Oro

671 To test the applicability of the SCOSSO RVS procedure for multi-hazard vulnerability prioritization, the city
 672 of Cagayan de Oro (CdeO) in the Philippines was chosen as a case-study. CdeO is a highly-urbanized city,
 673 situated along the north central coast of the Mindanao island (8°29'N 124°39'E) and facing Macajalar Bay
 674 with 25 kilometres of coastline. According to the 2015 census (CPH, 2015), the city has a population of
 675 675,950 and a population density of 1,600 p/km², making it the 10th most populous city in the Philippines.

676 In general, the city is exposed to extreme weather conditions resulting in storms and flood. While CdeO lies
 677 outside the typhoon belt, it is affected by the inter-tropical convergence zone. In December 2011, the tropical
 678 storm Washi hit CdeO, causing strong floodwater current swiping away mainly poor and social housing
 679 communities along the river banks, leaving about 2,000 people dead or missing, and resulting in more than
 680 US\$29.5M of damage (Sealza & Sealza, 2014). The recorded 24-hour rainfall at Lumbia, CdeO weather
 681 station, exceeded its monthly average by 60% reaching up to 180.9 mm. In terms of seismic hazards, CdeO
 682 is surrounded by Sulum, Philippine and Cotabato trenches, and relatively close to some major active seismic
 683 faults such as the Tagoloan and Davao river faults. The 2013 Bohol earthquake M7.2, was also felt in CdeO,
 684 although without causing damage.

685 A total of 115 school buildings have been visually surveyed in four days. All the surveyed structures are in
 686 elementary grade campuses in different locations of CdeO as indicated in Figure 13. A number of surveyed
 687 buildings are designated as disaster shelters. In each school campus, a mixture of buildings with various
 688 construction years, material, structural system, and function co-exists. As expected, a variation in the type of
 689 materials, workmanship and technology during the construction was observed, even in case of identical
 690 buildings. The survey results (Figure 14) indicate that the structural type of the surveyed buildings ranges
 691 from masonry to reinforced concrete (RC) framed structures. These are the majority at 70%. The typical
 692 number of storeys range between one to four storeys, with the single-story being the most common at 68%,
 693 similarly to the case of Nepal, illustrated in section 2.3. The roof structures are mainly steel (coupled with
 694 RC loadbearing frame), 51% or timber 41% (coupled with masonry loadbearing walls), with the majority in
 695 fair conditions (see Figure 15). The plan shapes in most cases varied from regular square to rectangular plan
 696 with a few rare cases of L-shaped, susceptible to torsional effects under earthquake action. Of the surveyed
 697 buildings, 23% were constructed after 2010, while up to 50% were built in the decades 1980s, 1990s and
 698 2000s. The construction year was obtained mainly from the school's registry documents or through
 699 interviewing locals. In a few cases (16%), the accurate built year could not be found and was indicated as
 700 unknown. As anticipated, signs of decay and poor structural conditions were observed in the structures which
 701 have been constructed over long periods of time.

702

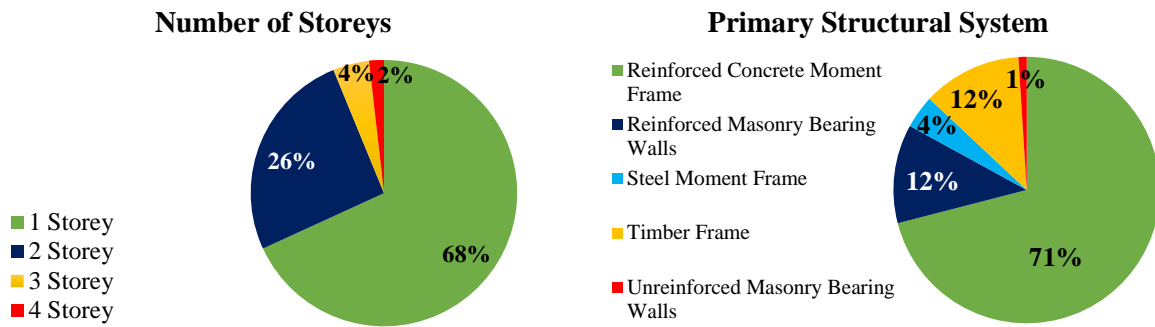


703

704

Figure 13. Geolocation of the surveyed school campuses

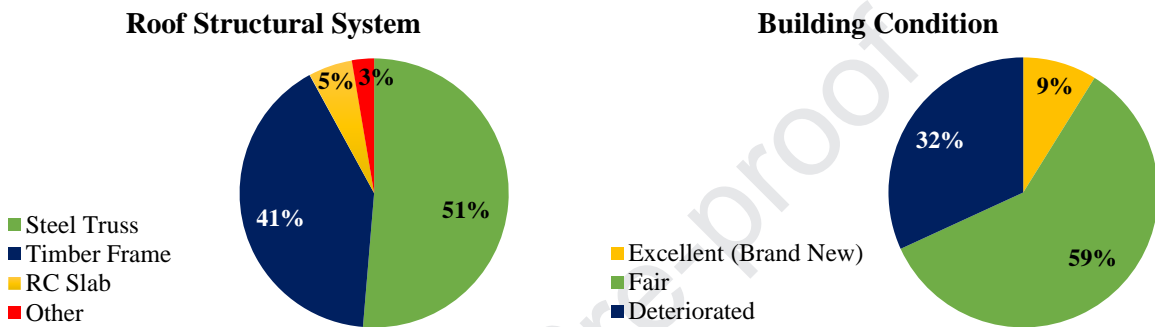
705



706

Figure 14. Distribution of stories and primary structural systems of schools in Cayan de Oro – Philippines

707



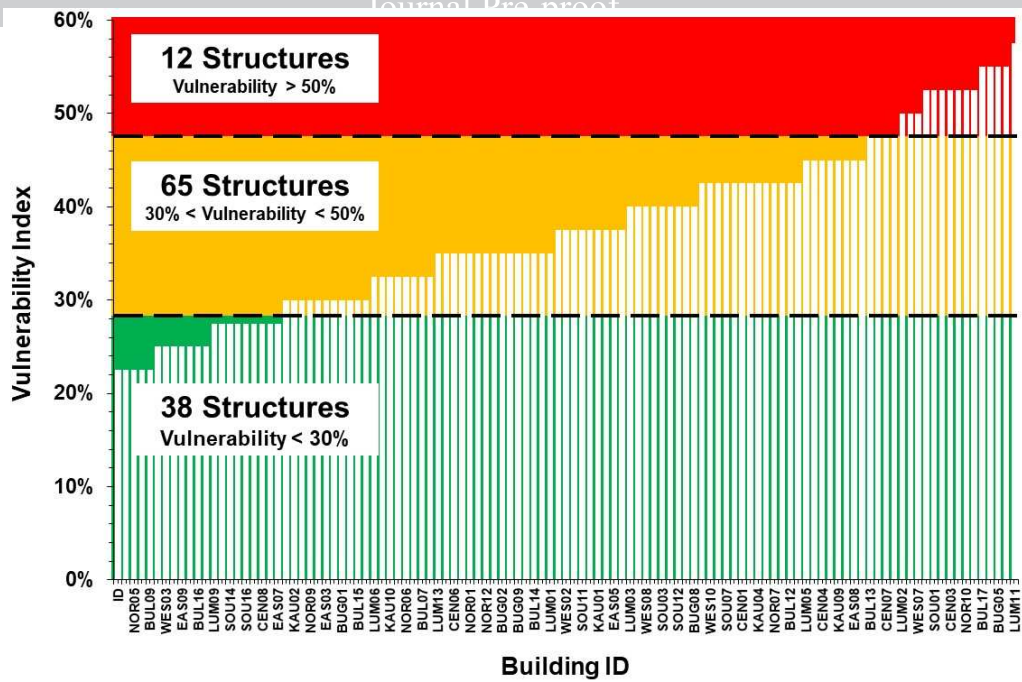
708

Figure 15. Distribution of roof structural systems and condition of schools in Cayan de Oro – Philippines

709

710 In most cases, the school buildings consist of rows of classrooms and a walkway or corridor in the
 711 longitudinal direction. Individual classrooms approximately measure $9\text{m} \times 7\text{m}$, with an approximate 3m
 712 wide walkway and typical floor height of 3m. The exposure assessment focused on the average number of
 713 student population per class, estimated at 40 to 50 pupils per classroom, considering the plan size and
 714 number of classrooms per structure. According to the collected data, the most common *index building*
 715 consists of a single storey RC frames with infill walls. The infill walls are mainly built with hollow concrete
 716 blocks with minimal contact between the infill and its surrounding frame. The buildings generally have
 717 gable-pitched roofs of twenty to thirty degrees, with purlins anchored in steel or wooden trusses to resist
 718 lateral and vertical loads from typhoon and seismic activity. Based on the collected vulnerable factors, due to
 719 the regular rectangular shape, the majority of surveyed buildings ($\approx 83\%$) are not susceptible to torsional
 720 effects. However, nearly half of the buildings ($\approx 43\%$) are prone to pounding effect due to the close proximity
 721 to nearby structures.

722



723

724

Figure 16. Vulnerability Index of 115 Surveyed Schools in Cayan de Oro – Philippines

725

726

727

728

For each school building, the surveyed data allows to determine its vulnerability index as explained in section 3.1. As shown in Figure 16, 26 structures (22.6%) have high overall vulnerability ($VI > 50\%$), hence a more detailed structural assessment and retrofitting/strengthening planning should be prioritized for these buildings.

729

730

731

732

733

734

735

The number of schools with moderate vulnerability is 78 (67.8%), while only 11 schools (9.56%) are characterized by a vulnerability index lower than 30%. The most vulnerable surveyed structure is KAU08 ($VI = 64.8\%$), i.e., a highly deteriorated masonry structure with unreinforced bearing walls, built in 1983, (Figure 17a). Similarly, BUL02 ($VI = 60.5\%$; Figure 17b) is a timber frame, single story, built in 1985, consisting of one classroom ($9m \times 4.8m$) with timber supports for its roof. The general condition of the structure as well as its roof and the connections have been described as deteriorated. In both cases, the buildings were susceptible to pounding effect and short column.

736



Figure 17. :a) Kauswagan Central (ID: KAU08); b) Bulua Central (ID: BUL02)

737

738

739

740

741

On the other hand, the structure with the lowest vulnerability index ($VI = 26\%$) is an isolated, brand new steel frame building (ID: WES12). The building consists of two storeys ($25.6m \times 6m$) and four classrooms in excellent condition and no report of obvious deficiencies (Figure 18a). Similarly, a RC building, 2 storeys high, (ID: SOU16) scored a vulnerability index of 29.9% (Figure 18b).



Figure 18: a) (ID: WES12); b) (ID: SOU16)

742 The building was built in 2012, consists of two floors and two classrooms with a steel truss roof. According
 743 to the collected data, the building is in an excellent condition with high-quality connections between the
 744 columns and the roof and no visible deficiency is observed. Figure 19, illustrates the individual VI values
 745 estimated for these four buildings with respect to each hazard and the average value. It can be seen that
 746 proportionally the highest vulnerability index is attained for either wind or flood hazard, while vulnerability
 747 of earthquake hazard is comparatively lower.

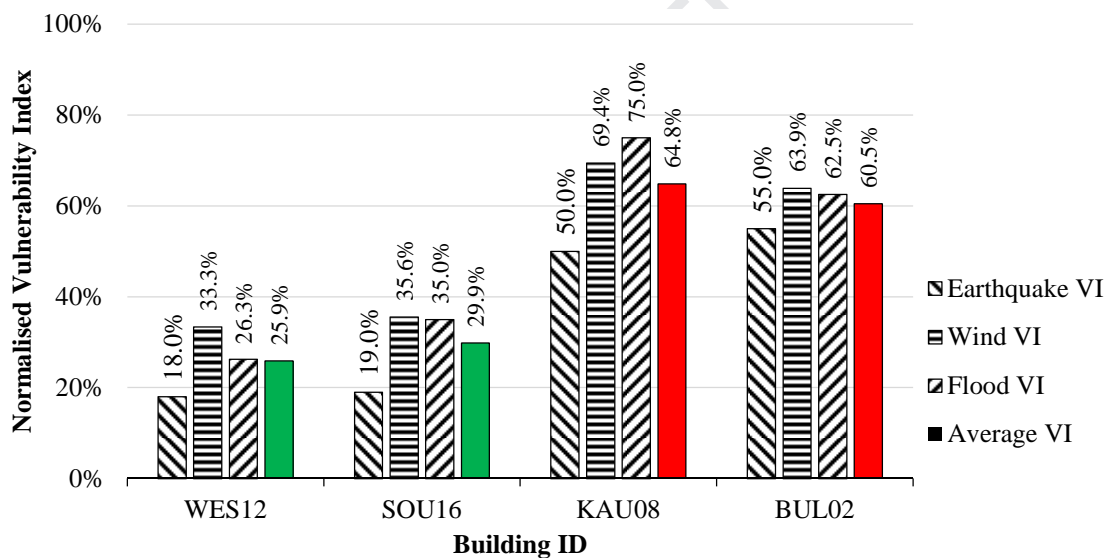


Figure 19. Hazard specific vulnerability index for selected buildings

748 The output of this simplified method based on RVS shows that it is possible to invest relatively modest
 749 resources to survey relatively large number of buildings in a short time and collect sufficient information to
 750 prioritise further analysis in relation to the exposure to a specific hazard and the specific building type. Given
 751 the modest number of typologies in any school building portfolio (Figure 14 and Figure 15) the results
 752 obtained for a small sample such as this one, are sufficient to underpin the application of different judgement
 753 criteria to identify the most vulnerable index buildings in the portfolio, to perform more accurate
 754 vulnerability assessment as discussed in section 2.3 and determine needs and best strategies for
 755 strengthening, as discussed in the next sections.

758 3.3. From rapid visual survey to retrofitting of school buildings

759 For the purpose of illustrating the process of fragility reduction when suitable strengthening strategy are
 760 chosen, two RC index buildings are chosen and their fragility assessment in relation to seismic hazard is
 761 conducted following the analytical approach highlighted in section 2. This choice is influenced by the
 762 consideration that seismic hazard is characterized by the highest impact/consequences (e.g., in terms of
 763

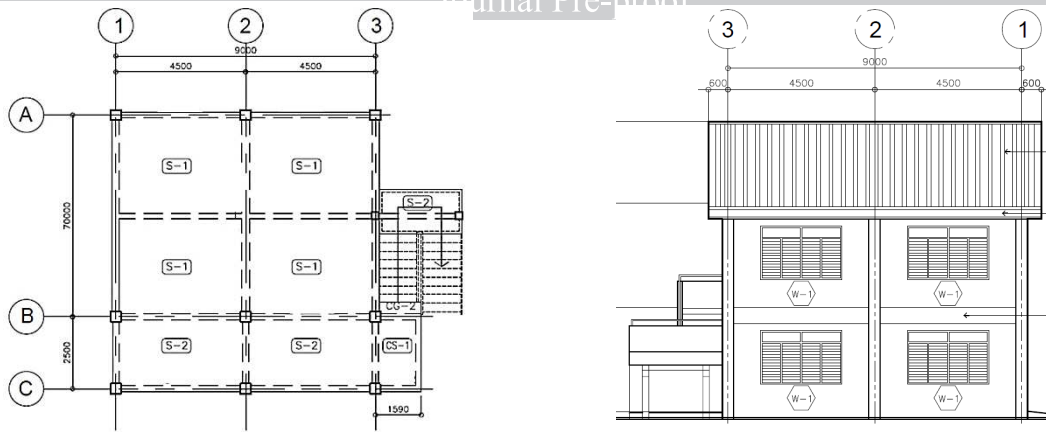
764 repair damage and casualties) with respect to other natural hazards, especially in the region of interest, for
765 comparable return periods. Moreover, seismic hazard can induce local/global collapse of buildings while
766 flood and wind hazards generally affect building content and non-structural components. For instance, the
767 October 2019 earthquake in Mindanao, about 100 kilometres away from Cagayan de Oro, have caused more
768 than 40 school building to suffer minor to considerable damage (Flores et al., 2019). Similarly, the April
769 2017 earthquake which hit Mindanao, caused damage to 14 schools in the provinces of Lanao del Sur and
770 Bukidnon, about 50 km away from Cagayan de Oro, according to the report prepared by National Disaster
771 Risk Reduction and Management Council of Philippines (NDRRMC, 2017).

772 It is also worth noting that approaches for physical vulnerability against wind and flood mainly rely on
773 empirical data – rather than engineering modelling (e.g., Dottori et al. (2016), Acosta et al., (2018)). Such
774 empirical data is not available for the region of interest and existing approaches are mainly based on expert
775 judgment (similar to the proposed index) The index building selection was conducted in a way to represent
776 some of the common typologies also according to the national school building inventory published by the
777 Philippines Department of Education in 2014.

778 The first building is a two storey RC frame, consisting of two classrooms, one per storey, with two bays and
779 three frames and it is the most common typology, besides the one storey buildings, but more vulnerable than
780 those to seismic action. The second structure includes 15 classrooms, distributed on three storeys, including
781 12 bays and three frames. The spacing of bays and frames of both building are similar with classrooms
782 having dimensions of $7\text{m} \times 9\text{m}$. Storey height is standard at 3.2m. The three-storey building has one of the
783 largest footprints ($\approx 1,540\text{m}^2$) among the typical school buildings in the Philippines. With an average of 45
784 students per classroom according to the survey observations, the building accommodates more than 675
785 students and teachers, making it a particularly exposed structure to ground shaking. This is considered the
786 highest damage consequence case, and hence high qualifier for performing the fragility assessment.
787 Although currently building of this size are a small minority, this typology is recommended for upper
788 primary and secondary schools as well, and, as the scholar population increases, it is being implemented in
789 several new school developments. The buildings do not include any staircase core or shear walls to result in
790 significant torsional effects. The plan and elevation of the selected index buildings are illustrated in Figure
791 20 and 21.

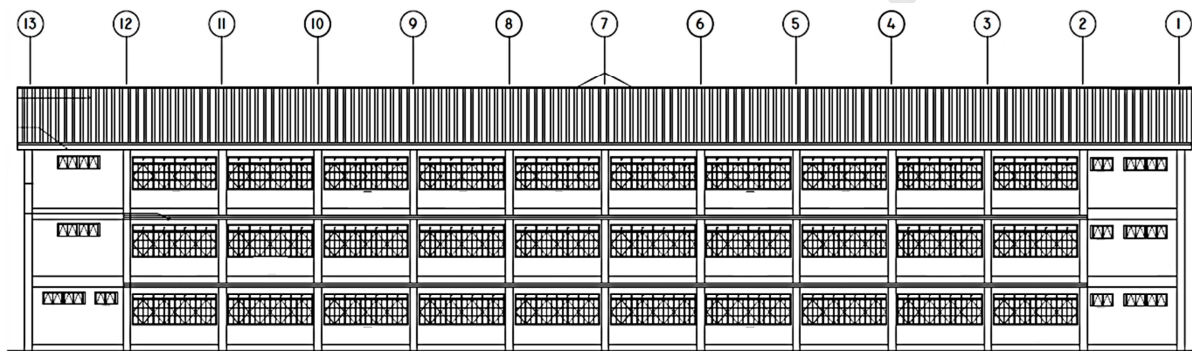
792 As the elevation indicates, the majority of walls and partitions consist of lightweight concrete hollow blocks
793 (150 mm CHB) with relatively large openings as entrance door or windows. Thus, the infill panels would not
794 have a considerable effect on the global capacity and initial stiffness of the structures. Therefore, as a way of
795 simplification, their effect is neglected in the numerical simulations. The unit weight of walls are added as
796 distributed loading on the beams. The material characteristics and section arrangements are defined
797 following a statistical analysis of the schools' detailed drawing, made available by Philippines' Department
798 of Education (DepEd), as well as the local design code provisions. For beams, columns and slabs, a concrete
799 with mean strength value of 28 MPa is implemented, reinforced with ribbed steel bars with a mean strength
800 of 253 MPa. All members have 40 mm cover and have similar arrangement of longitudinal reinforcement.
801 The shear bars are $\phi 10$ with spacing of 0.2 m. An imposed load of 1.9 kN/m^2 for the classrooms and 3.2
802 kN/m^2 for the corridors are applied according to the National Structural Code of the Philippines, Volume 1
803 (NSCP 2015). The tributary area for the beams was assumed to follow a simplified triangular distribution, as
804 the reinforcement arrangement in the slabs allows this load path to be achieved.

805 Three dimensional nonlinear models of the index buildings are developed using the fiber-based finite
806 element software SeismoStruct (2016). The software is capable of predicting large displacement behaviour
807 of space frames under static and dynamic loadings, taking into consideration the geometric non-linearities
808 (e.g. P- Δ and P- δ) and material inelasticity. It accounts for the spread of inelasticity along the members'
809 length and across the sections' depth. The materials models are appropriately chosen from the Seismostruct
810 library to represent reinforcing steel bars, concrete and FRP confined concrete. The slab modelling is carried
811 out by implementing rigid diaphragms at each floor and the slab's loads are transformed to masses and
812 applied directly to the beams that support the slab. As the structural behaviour is predominantly influenced
813 by the first period of vibration and mode shape, the nonlinear static pushover (SPO) procedure is a reliable
814 mean of obtaining the structural response, according to the Guidelines set out in GLOSI, as already
815 mentioned in section 2.3 and further discussed in detail in D'Ayala et al (2015).



817 **Figure 20. Plan (left) and elevation (right) view of the 2-storey, 2-classroom school (DepEd, 2012)**

818



819 **Figure 21. Elevation view of 3-storey, 15-classroom school (DepEd, 2012)**

820

821

822 In this study, the SPO analysis is conducted to failure, with incremental uniform load distribution and an
 823 inverted triangular distribution, performed independently for both longitudinal and transversal direction of
 824 the building in order to identify the weaker direction. Response control was utilised for the loading phase and
 825 terminated the analysis once the control node, located at mass centre of the roof, reaches a drift of 0.3 metre,
 826 according to FEMA 356 (2000). This loading strategy is able to identify any irregular response features (e.g.
 827 soft storey), capture the softening post-peak branch of the response and obtain an even distribution of points
 828 on the force-displacement curve. The structural response is obtained in terms of base shear versus top
 829 displacement and it is used to compute the fragility function as illustrated in section 2.3. The SPO analysis
 830 identifies for both building as main deficiency a lack of sufficient flexural capacity and confinement for all
 831 ground columns, eventually leading to soft-storey failure of the structure. The capacity of each column has
 832 been evaluated separately, according to the provisions of the National Structural Code of the Philippines,
 (NSCP, 2015).

833 Among different strengthening strategies, strengthening the beams and columns with FRP wrapping is
 834 considered to be the most efficient and least disruptive to improve the overall structural performance by
 835 increasing the structural capacity and ductility through column confinement. In recent years, this type of
 836 intervention has become common in several earthquake-prone regions around the world due to high strength
 837 to weight ratio of the FRP fabric, high mechanical properties, corrosion resistance and most notably its speed
 838 of implementation (e.g., De Lorenzis and Tepfers 2003; Wu et al. 2006). Several examples of FRP
 839 retrofitting have been reported in the aftermath of the 2009, L'Aquila earthquake, Italy, selected for its
 840 reduced installation time, allowing quick re-opening of the schools, while significantly increasing the seismic
 841 capacity of the building (Fracadore et al., 2015).

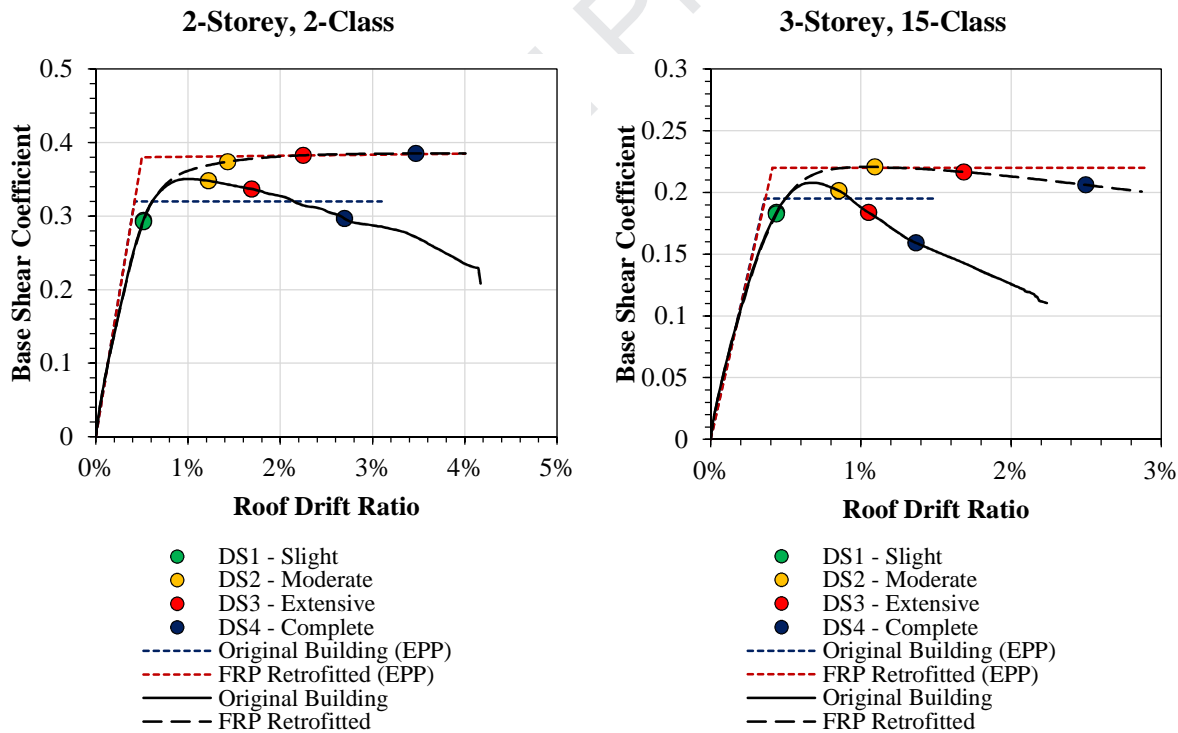
842 In general, FRP is considered expensive when compared to other retrofitting strategies such as concrete
 843 jacketing, steel bracing and the introduction of shear walls. However, the FRP wrapping is preferred in cases
 844 where there is limited access to the structure or minimal disruption is required (e.g., FEMA-547, 2006). FRP
 845 wrapping can address deficiencies related to inadequate shear and flexural capacity, as well as enhancing the
 846 concrete behaviour, thanks to enhanced confinement. Depending on the case, due to the positioning of wall
 847 partitions, ceilings and/or other architectural or structural elements, accessing structural members to apply

848 the FRP wrapping may be challenging. Therefore, local removal of structural members, such as the slab, may
 849 be required, particularly in case of beam-column joints. Furthermore, the potential slab interaction with the
 850 strengthened member is to be considered in the design and analysis stage, as this may affect strengthening
 851 requirements or placing a gap to prevent interaction (e.g., FEMA-547, 2006).

852 For this study, the main aim was to increase the ductility and member strength following the observations of
 853 the nonlinear analysis. Referring to the structural analysis, the weakest beams and columns were identified
 854 and the FRP wrapping were designed accordingly to the guidelines of CNR-DT 200.1R-13 (CNR, 2014),
 855 while following the preferred capacity hierarchy of strong column-weak beam (ASCE 41-13, 2013, NSCP,
 856 2015). Furthermore, the design explicitly incorporated the optimal bond length, efficiency of confinement
 857 and orientation of fibers. The chosen FRP for all beams and columns is the commercial SikaWrap Hex 103C,
 858 selected based on availability in the region under study.

859 The comparison of pushover curves obtained for both buildings before and after retrofitting is illustrated in
 860 Figure 22, in terms of base shear coefficient (base shear/mass) and roof drift ratio (top drift/total height). The
 861 main improvement in performance obtained in both cases by installation of FRP is an increase of 9.9% and
 862 6.2% in terms of strength for the 2-storey and 3-storey buildings respectively. In terms of ductility, if the
 863 ratio of drift at the ultimate strength (δ_{ult}) to that of yield strength (δ_{yld}) is considered, an increase of about
 864 358% in case of the 2-storey and an increase of 55% for the 3-storey building is observed.

865 As discussed above, fragility functions are one of the fundamental tools in assessing seismic risk, describing
 866 the probability of exceeding different damage limit states for a given level of ground shaking. To derive
 867 fragility function for this study, the FRACAS (Fragility through Capacity Spectrum Assessment; Rossetto et
 868 al., 2016) methodology has been chosen. This differs slightly from the N2 procedure adopted in GLOSI (see
 869 section 2.3) by the way in which it identifies the performance points. Nassirpour and D'Ayala (2018) have
 870 shown that there is modest difference between the results obtained with the two methods for this type of
 871 buildings.



872 **Figure 22. Static pushover curve of the analysed structures before and after retrofitting**

873

874 The capacity curve obtained for each structure, before and after retrofitting, has been idealised using a
 875 bilinear elastic perfectly plastic (EPP) curve, as illustrated in Figure 22 and already discussed in section 2.3.
 876 However, in this case the ground motion intensity is characterized by the spectral pseudo-acceleration
 877 corresponding to the first-mode elastic vibration period and 5% damping ratio ($S_d(T_1)$) rather than PGA, as
 878 shown for the masonry building in the previous section. Spectral acceleration is a perfect predictor for the
 879 response of elastic SDoF systems and a relatively good predictor for MDoFs, in case their response is

880 dominated by the fundamental mode of vibration (Shome et al., 1998), as the structures investigated here.
 881 As already introduced in section 2.3, the far-field ground motion set suggested in FEMA P-695 (FEMA,
 882 2009) has been used to compute the performance points. Differently from the GLOSI application, as in this
 883 case the study is location specific, the mean spectrum of the ground motions has been verified for agreement
 884 with the code-based design response spectrum of Philippines as prescribed in NSCP (2015). The soil profile
 885 of Cagayan de Oro can be categorized as very dense soil and soft rock ($360 < V_{s,30} \leq 760$) and according to
 886 seismic zonation of the code, CdeO is located in zone IV with faults that are capable of producing large
 887 magnitude events ($M \geq 7.0$) and have a high rate of seismic activity indicating a peak ground acceleration of
 888 0.4g. To ensure the records can trigger a vast range of structural responses, from elastic to nonlinearity and
 889 collapse, a scaling factor from 0.25 to 2.25 for the ordinates has been introduced to each selected record.

890 A critical stage of fragility function derivation includes characterizing appropriate damage states and
 891 allocating rational global and local damage states. For the structure under study, maximum inter-storey drift
 892 ratio (MIDR) is employed as the engineering demand parameter (EDP), a quantifiable global indicator for
 893 each damage state. MIDR is a suitable choice for moment-resisting frames, since it relates the global
 894 response of the structure to joint rotations, in which most of the inelastic behaviour of a moment resisting
 895 frame (MRF) is concentrated. In order to define appropriate damage states, the recommendations of a
 896 number of guidelines and codes such as HAZUS-MH MR4 (2003), HRC (Rossetto & Elnashai, 2003) and
 897 VISION 2000 have been reviewed.

898 The selected damage thresholds in terms of MIDR, employed for the fragility curves derivation are presented
 899 in Table 3, along with a brief description of the corresponding damage state. Similar to the thresholds
 900 suggested by HAZUS for low- and mid-rise moderate code reinforced concrete MRF, which are identical, in
 901 this study the same damage threshold values are utilised for both considered buildings. As the impact of FRP
 902 on the initial stiffness and period of the structure is minor, the initial damage state (slight) will be identical
 903 for both cases. The most distinction in thresholds is observed in case of complete damage state, for which,
 904 the FRP retrofitting has considerably improved the ductility of both structures and hence the structure can
 905 withstand higher deformation prior to failure. Similarly, for moderate and extensive damage states, the
 906 threshold has shifted as the structure's capacity and ductility has improved after the retrofitting is
 907 implemented.

908 **Table 3. Description of damage limit states and the assigned damage thresholds**

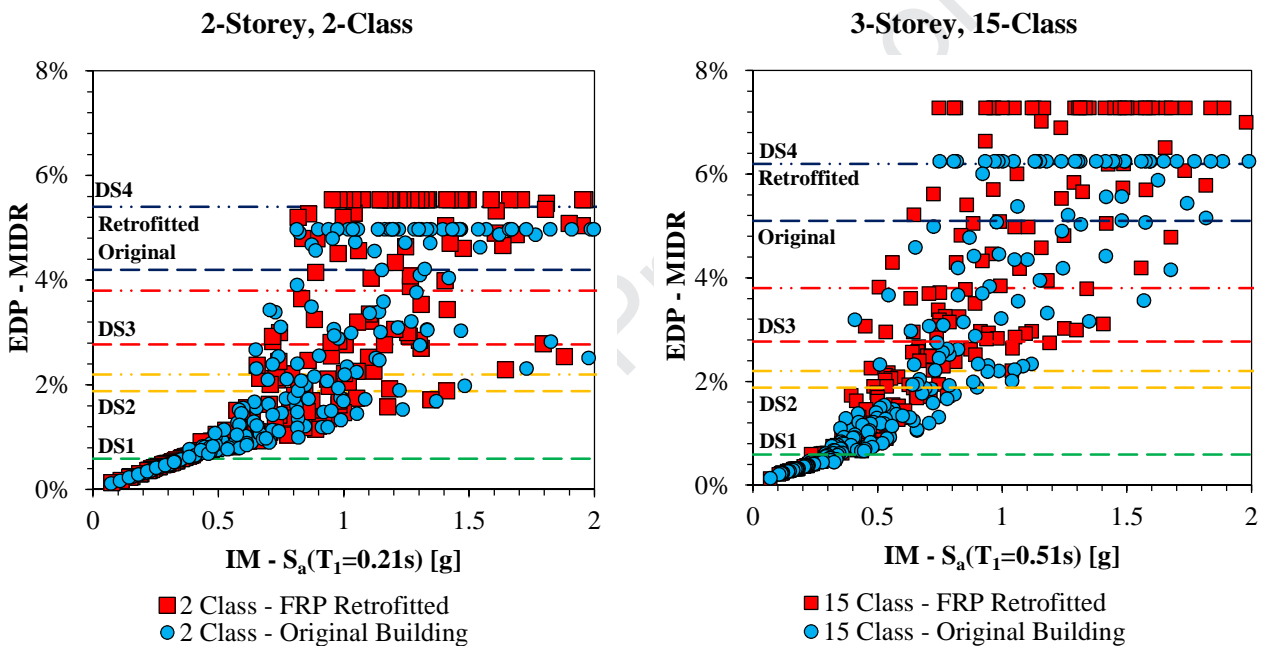
Damage Limit State	Performance Level	Description	Damage Threshold (MIDR)	
			Original Building	FRP Retrofitted
<i>DS1 - Slight</i>	Operational	Elastic behaviour of components. Limited yielding to a few members. No crushing of concrete (confined or unconfined).	0.59%	0.59%
<i>DS2 - Moderate</i>	Immediate Occupancy	Concrete cover spalling at several locations for columns and beams (i.e. crushing of unconfined concrete).	1.88%	2.20%
<i>DS3 - Extensive</i>	Life safety	Extensive crushing in some columns and/or beams at different floors, few concrete core crushing in columns. Max allowable FRP rupture strain = 0.016	2.77%	3.80%
<i>DS4 - Complete</i>	Collapse prevention	More than 40% of crushing in some columns and/or beams. Shear failure or total failure/cracking of columns and beams.	4.20%	5.40% [2 Class]
			5.10%	6.20% [15 Class]

909

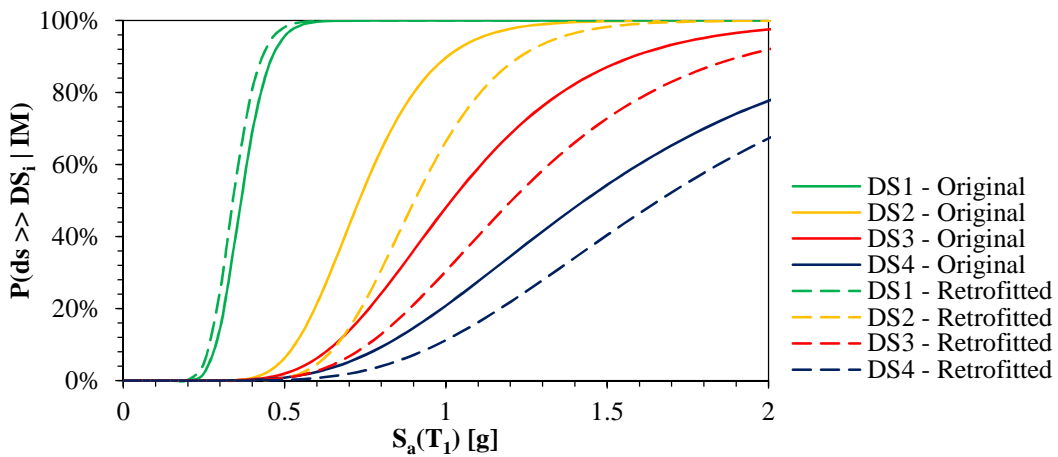
910 The outcome of FRACAS analysis is presented in terms of IM versus EDP for both structures before and
 911 after retrofitting. The obtained IM-EDP points along with the allocated damage thresholds of the original and
 912 retrofitted buildings are illustrated in Figure 23. The number and scaling of earthquake records, imply that

913 240 nonlinear dynamic runs were carried out for each model in FRACAS. The results indicate an
 914 improvement in performance of the structure after the FRP wrappings are implemented. Therefore, due to the
 915 enhancement in ductility and capacity, for a certain value of acceleration applied, the retrofitted structure can
 916 undergo a larger deformation. As expected the elastic performance of the structure at both phases are
 917 identical, similar to the results observed in the nonlinear static pushover.

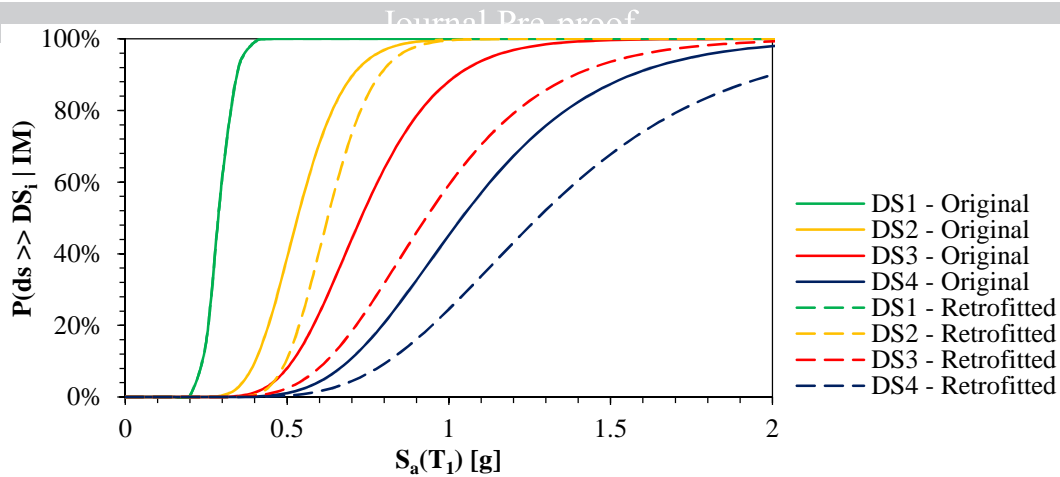
918 In order to derive the fragility functions for the IM-EDPs generated by the simplified method, a generalized
 919 linear regression method (GLM) with clog-log link function (Basöz & Kiremidjian, 1998) have been applied
 920 to the performance points obtained through FRACAS. A thorough discussion of different regression
 921 procedures commonly used for developing fragility functions can be found in Lallemand et al. (2015) and
 922 Baker (2015). The fragility curves obtained for both structures before and after retrofitting are compared in
 923 Figure 24 and 25. As expected, the fragility curves representing the retrofitted structure have higher median
 924 for all damage states except the slight. The reason is the fact that FRP does not impact the structure's
 925 stiffness and capacity up to this threshold, hence the structure behaves as its original state. The improvement
 926 observed in the performance of the structure after implementing FRP retrofitting, indicates lower
 927 vulnerability and damage ratio, which can consequentially result in a reduction of social and economic
 928 losses.



929 **Figure 23. IM-EDP results obtained from FRACAS along with the damage thresholds implemented**
 930 **for the original building**



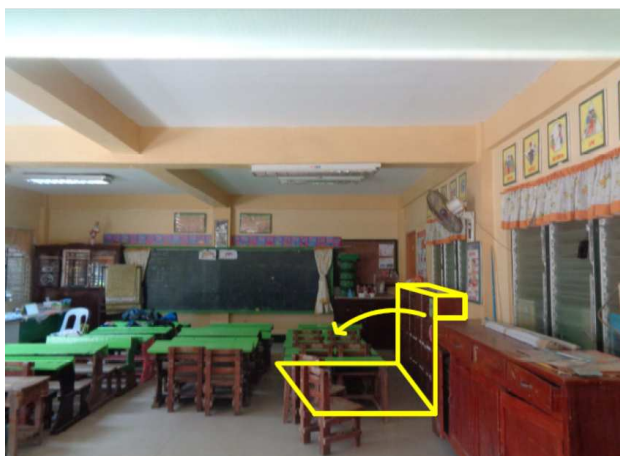
931
 932 **Figure 12. Comparison of fragility curves obtained for 2 Storey – 2 Class before and after FRP**
 933 **retrofitting**



934
935 **Figure 25. Comparison of fragility curves obtained for 3 Storey – 15 Class before and after FRP**
936 **retrofitting**

937
938 **3.4. Reducing non-structural vulnerability**

939 Alongside the structural fragility and vulnerability assessment of the school structures, the non-structural
940 components of the surveyed school facilities have been investigated to identify the potential risks to the
941 safety of the occupants. A guideline is prepared consisting of retrofitting measures to reduce any potential
942 risk of injury or death due to falling, overturning, shifting or rearrangement of the equipment and facilities
943 existing in the class rooms as shown in Figure 26. Special care is spent on evacuation routes and making sure
944 no obstruction is caused during any of the considered hazards.



946 **Figure 26. Assessment of non-structural components of the school infrastructure and identifying potential issues**

947 As part of both the GLOSI and the Philippines projects, several training and capacity building sessions have
 948 been organised in the countries under study in order to disseminate the culture of safe schools. Local
 949 engineers, disaster responders, stakeholders and decision makers have been invited to two-to-three day-long
 950 workshops, in which the state-of-the-art techniques and methods on structural and non-structural
 951 vulnerability assessment and resilience enhancement are discussed (Figure 27). The training composes of
 952 lecture notes on relevant basic and advanced concepts, as well as several hours of multimedia material,
 953 demonstrating step-by-step assessment process using the latest applicable software.



954 **Figure 27. Workshops on vulnerability and resilience of schools against natural hazards**

954

955

956

Conclusions

957 Taking into consideration the high probability of occurrence for various natural hazards across the world,
 958 and particularly in developing countries, assessing multi-hazard vulnerability and risk of school buildings is
 959 an urgent task for governmental authorities and first responders. Given the large number of existing school
 960 sites and their geographical distribution, appropriate and effective tools and approaches are required to
 961 address the prevailing physical and social vulnerabilities of the school infrastructure to multiple natural
 962 hazards at global scale. Specifically, developing a comprehensive dataset of typical and systematically
 963 defined structural typologies for schools, including main structural and non-structural characteristics (e.g.,
 964 age of construction, number of story, lateral load resisting system and materials, number of occupants),
 965 common defects, typical damage associated to multiple natural hazards, is beneficial for disaster
 966 management planning and decision making along with prioritization and resource allocation for
 967 retrofitting/strengthening plans for such structures. This basic information needs to be collected and analyzed
 968 in a consistent and standardized form, if it is to be used in the development of Risk Mitigation Programmes,
 969 allowing to define needs at country and regional levels. The methodology developed within the GPSS
 970 programme with the GLOSI initiative has made strides in this direction, indicating that it is possible to
 971 determine a uniform taxonomy systems, that can includes all type of typologies and account for various level

972 of available information. The identification of index buildings following such approach allows to define
973 seismic fragility and vulnerability functions for specific typologies of general applicability, using relatively
974 simple analytical models, at the reach of most graduates of civil engineering programmes including seismic
975 engineering tuitions. As shown in the application case study of CdO the fragility assessment method applied
976 is able to quantify the reduction in fragility afforded by strengthening.

977 Moreover, a series of tools for a rapid yet reliable visual multi-hazard vulnerability prioritization of school
978 infrastructure against potentially destructive natural hazards, i.e., earthquake, typhoon, and flood, have also
979 been tested. The rapid visual survey mobile application allows to categorize the buildings in terms of the
980 primary indicators identified for the GLOSI taxonomy, and also compute simplified vulnerability indices to
981 swiftly determine the safety level of the considered buildings. To test the applicability of the proposed tools,
982 115 school buildings in Cagayan de Oro have been surveyed and their vulnerability indices have been
983 estimated. This has been followed by the selection of two index buildings and the derivation of analytical
984 fragility relationships. To mitigate the identified structural deficiencies and improve the overall seismic
985 performance of the two case-study structures, structural and nonstructural retrofitting measures have been
986 proposed. The results of the analysis indicated a considerable improvement in the overall seismic
987 performance of each considered structural system, particularly as the structure enters its inelastic behavior.

988 The proposed tools represent a first step toward a detailed multi-hazard risk and resilience assessment
989 framework of school infrastructure. The aim is to allow stakeholders and decision-makers to quickly identify
990 the most vulnerable structures among the surveyed stock, to guide more detailed data collection campaigns
991 and structural assessment procedures (e.g., analytical vulnerability approaches, through fragility and
992 vulnerability relationships), and ultimately to plan further retrofitting/strengthening measures or, if
993 necessary, school replacement/relocation.

994

995

996 **Acknowledgement**

997 The authors gratefully acknowledge the support of several funding agencies which has underpinned the
998 development of the work reported in this article: to The World Bank for funding the GLOSI project, the
999 University College London (UCL) Global Challenges Research Fund (GCRF) Small Research Grants
1000 scheme for funding the SCOSSO project, the British Council Newton Fund Institutional Links for funding
1001 the PRISMH project.

1002

1003

References

- 1004
1005
1006 ACAPS (2014), “Typhoon Yolanda, Secondary Data Review - January 2014”, Humanitarian Response, OCHA
1007 Services, ACAPS Report, Philippines.
- 1008 Acosta T.J.S., Galisim J.J., Tan L.R., Hernandez J.Y., (2018), “Development of Empirical Wind Vulnerability Curves
1009 of School Buildings Damaged by the 2016 Typhoon Nina”, *Procedia Engineering*, Vol. 212.
- 1010 Adhikari, R. K. and D'Ayala, D (2019), Applied Element Modelling and Pushover Analysis of Unreinforced Masonry
1011 Buildings with Flexible Roof Diaphragm. In: Proceedings of the 7th International Conference on Computational
1012 Methods in Structural Dynamics and Earthquake Engineering (COMPdyn 2019), Crete, Greece.
- 1013 Adhikari, R., Yadav, R.B., Jha, S., Thapa, M., Cortez, F.R., Ferreira, C.F. and Shrestha, B.C. (2016) Structural Integrity
1014 and Damage Assessment for Educational Infrastructures in Nepal, Phase I: Results and Finding. SIDA Report, The
1015 World Bank, Washington D.C., USA
- 1016 Adhikari, R.K., D'Ayala, D.F., Ferreira, C.F., Cortez, F.R. (2018), Structural Classification System for Load Bearing
1017 Masonry School Buildings. In: Proceedings of 16th European Conference on Earthquake Engineering (16ECEE),
1018 Thessaloniki, Greece.
- 1019 ASCE/SEI 41-13, 2013. Seismic Evaluation and Retrofit of Existing Buildings. American Society of Civil Engineers,
1020 Reston, Virginia - United States of America.
- 1021 ASI (2018) Extreme Loading for Structures, Applied Science International, LLC, North Carolina, USA.
- 1022 Associated Press. Sichuan earthquake killed more than 5,000 pupils, says China. *The Guardian*, [online]. 2009 May. Available
1023 at: <https://www.theguardian.com/world/2009/may/07/china-quake-pupils-death-toll>
- 1024 ATC (1985) ATC-13 Earthquake Damage Evaluation Data for California. Applied Technology Council, USA.
- 1025 Baker JW (2015): Efficient Analytical Fragility Function Fitting Using Dynamic Structural Analysis. *Earthquake*
1026 *Spectra*, Volume 31, Issue 1, pp.579-599.
- 1027 Basoz N and Kiremidjian AS (1998), “Evaluation of Bridge Damage Data from the Loma Prieta and Northridge,
1028 California Earthquake,” Technical Report MCEER-98-0004, Multidisciplinary Center for Earthquake Engineering,
1029 State University of New York, Buffalo, NY, USA
- 1030 Brzev S., Scawthorn C., Charleson A.W., Allen L., Greene M., Jaiswal K., and Silva V. (2013), “GEM Building
1031 Taxonomy (Version 2.0)”, GEM Technical Report 2013-02, GEM Foundation.
- 1032 Census of Population and Housing (CPH) (2015) "Region X (Northern Mindanao)". Total Population by Province, City,
1033 Municipality and Barangay. Philippines Statistics Authority (PSA).
- 1034 CNR (2014). Guide for the Design and Construction of Externally Bonded FRP Systems for Strengthening Existing
1035 Structures.
- 1036 Coburn A. and Spence R., (2002), “Earthquake Protection”, John Wiley & Sons Ltd., England.
- 1037 D'Ayala, D., Meslem, A., Vamvatsikos, D., Porter, K., Rossetto, T. (2015) Guidelines for Analytical Vulnerability
1038 Assessment - Low/Mid-Rise. GEM Technical Report, GEM Foundation, Pavia, Italy.
- 1039 De Lorenzis, L. and Teppers, R. (2003). Comparative study of models on confinement of concrete cylinders with fiber-
1040 reinforced polymer composites, *Journal of Composites for Construction*, ASCE, 7(3): 219-237.
- 1041 Dhungel R., Guragain R., Joshi N., Pradhan D., Acharya S.P., (2012), “Seismic Vulnerability Assessment of Public-
1042 School Buildings In Nawalparasi And Lamjung District Of Nepal.”, 15 World Conference on Earthquake Engineering,
1043 Lisbon, Portugal.
- 1044 Dottori, F., Figueiredo, R., Martina, M. L. V., Molinari, D., and Scorzini, A. R., (2016), “INSYDE: a synthetic,
1045 probabilistic flood damage model based on explicit cost analysis”, *Nat. Hazards Earth Syst. Sci.*, 16, 2577–2591,
1046 <https://doi.org/10.5194/nhess-16-2577-2016>, 2016.
- 1047 DRES, (2017), “A preliminary report on school buildings performance during M 7.3 Ezgeleh, Iran earthquake of
1048 November 12, 2017”, Organization for Development, Renovation and Equipping Schools of I.R.Iran (DRES).
- 1049 Fajfar, P (2000) A nonlinear analysis method for performance-based seismic design. *Earthquake Spectra* 16.3: 573-592.
- 1050 FEMA, (2000). FEMA-356: Pre-standard and Commentary for the Seismic Rehabilitation of Buildings. Rehabil.
1051 Requir. 1–518.
- 1052 FEMA, (2006). FEMA-547: Techniques for the Seismic Rehabilitation of Existing Buildings, Federal Emergency
1053 Management Agency, Washington D.C.
- 1054 FEMA, (2009). FEMA P-695: Quantification of Building Seismic Performance Factors, Federal Emergency
1055 Management Agency, Washington D.C.
- 1056 FEMA, (2012) FEMA P-58-1: Seismic Performance Assessment of Buildings, Volume 1 – Methodology, Federal
1057 Emergency Management Agency, Washington D.C.
- 1058 Flores H., Mateo J., Unson J., Laude J., (2019), “40 schools damaged in Mindanao quake”, Link:
1059 <https://www.philstar.com/headlines/2019/10/19/1961527/40-schools-damaged-mindanao-quake>.
- 1060 Frascadore R, Di Ludovico M, Prota A, Verderame GM (2015). Local strengthening of reinforced concrete structures as
1061 a strategy for seismic risk mitigation at regional scale. *Earthquake Spectra*. 31 (2), 1083–1102.
- 1062 GPDRR, (2009) Creating Linkages for a Safer Tomorrow, Global Platform for Disaster Risk Reduction, Proceedings:
1063 Second Session of the Global Platform for Disaster Risk Reduction, Available online at
1064 <https://www.preventionweb.net/globalplatform/2009/> (accessed on 01 July 2019).

- 1065 Gentile, R. and Galasso, C. (2019), From rapid visual survey to multi-hazard risk prioritisation and numerical fragility
1066 of school buildings in Banda Aceh, Indonesia, *Nat. Hazards Earth Syst. Sci. Discuss.*, [https://doi.org/10.5194/nhess-](https://doi.org/10.5194/nhess-2018-397)
1067 2018-397.
- 1068 Grant D. N, Bommer, J.J., Pinho, R., Calvi, G.M. Goretti, A., Meroni, F.(2007), “A Prioritization Scheme for Seismic
1069 Intervention in School Buildings in Italy.” *Earthquake Spectra*: May 2007, Vol. 23, No. 2, pp. 291-314.
- 1070 Grünthal, G. (Ed.) (1998) *European Macroseismic Scale 1998 (EMS-98)* European Seismological Commission, sub
1071 commission on Engineering Seismology, Working Group Macroseismic Scales. Conseil de l’Europe, Cahiers du Centre
1072 Européen de Géodynamique et de Séismologie, Vol. 15, Luxembourg.
- 1073 Guragain, R. (2015), *Development of Earthquake Risk Assessment System for Nepal*, PhD thesis, The University of
1074 Tokyo, Japan.
- 1075 IFRC, (2016), “Philippines: Typhoon Haiyan, Three-year progress report”, International Federation of Red Cross and
1076 Red Crescent Societies, Manila, Philippines.
- 1077 International Financial Corporation, 2010, *Disaster and Emergency Preparedness: Guidance for Schools*, World Bank Group.
1078 <https://www.ifc.org/wps/wcm/connect/8b796b004970c0199a7ada336b93d75f/DisERHandbook.pdf?MOD=AJPERES>
- 1079 International Institute for Sustainable Development, (2009), *A Summary Report of the Second Session of the Global Platform
1080 for Disaster Risk Reduction*, GPDRR Bulletin, VOLUME 141, NUMBER 2, p.12 MONDAY, 22 JUNE 2009,
1081 <http://enb.iisd.org/download/pdf/sd/ymbvol141num2e.pdf> (accessed on 01 July 2019)
- 1082 Jaiswal K. and Wald D.J., (2008), “Creating a Global Building Inventory for Earthquake Loss Assessment and Risk
1083 Management.”, U.S. Geological Survey, Reston, Virginia.
- 1084 Jaiswal K.S., Wald D.J., Earle P.S., Porter K.A., Hearne M. (2011) *Earthquake Casualty Models Within the USGS
1085 Prompt Assessment of Global Earthquakes for Response (PAGER) System*. In: Spence R., So E., Scawthorn C. (eds)
1086 *Human Casualties in Earthquakes*. *Advances in Natural and Technological Hazards Research*, vol 29. Springer,
1087 Dordrecht
- 1088 Jaiswal, K., Wald, D. and D’Ayala, D., (2011) *Developing empirical collapse fragility functions for global building
1089 types*. *Earthquake Spectra*, 27(3), pp.775-795.
- 1090 Jaiswal, K.S. and Wald, D.J., (2008) *Creating a Global Building Inventory for Earthquake Loss Assessment and Risk
1091 Management*. U.S. Geological Survey Open-File Report 2008-1160, 103 p.
- 1092 Lagesse, R., Rossetto, T., Raby, A., Brennan, A., Robinson, D., Adhikari, R.K., Rezki-Hr, M., Meilianda, E., Idris, Y.,
1093 Rusydy and I., Kumala, I.D. (2019) *Observations from the EEFIT-TDMRC Mission to Sulawesi, Indonesia to
1094 Investigate the 28th September 2018 Central Sulawesi Earthquake*, SECED 2019 Conference, London, United Kingdom.
- 1095 Lallemand, D., Kiremidjian, A., Burton, H., (2015) *Statistical procedures for developing earthquake damage fragility
1096 curves*, *Earthquake Engineering & Structural Dynamics*, Vol.44, Issue 9, pp. 1373–1389.
- 1097 MARN (2012) *Modelacion Probabilistica de Escenarios de Reisgo Sismico Para el Area Metropolitana de San Salvador*,
1098 *Incluye Analisis de Los Portafolios de Educacion, Salud y Gobierno*. Ministerio de Medio Ambiente y Recursos
1099 Naturales, El Salvador. (In Spanish)
- 1100 Nassirpour A, Galasso C, D’Ayala D (2017). *SCOSSO: Safer Communities through Safer Schools*. EPICentre Internal
1101 Report, University College London, United Kingdom.
- 1102 National Disaster Risk Reduction and Management Council of Philippines (NDRRMC), (2017), “SitRep No. 09 M 6.0
1103 Earthquake in Wao, Lanao del Sur”. Link:
1104 [http://www.ndrrmc.gov.ph/attachments/article/3059/Update_on_Sitrep_No_09_Re_Magnitude_6_0_Earthquake_in_W](http://www.ndrrmc.gov.ph/attachments/article/3059/Update_on_Sitrep_No_09_Re_Magnitude_6_0_Earthquake_in_Wao_Lanao_Del_Sur_as_of_20April2017_8AM.pdf)
1105 [ao_Lanao_Del_Sur_as_of_20April2017_8AM.pdf](http://www.ndrrmc.gov.ph/attachments/article/3059/Update_on_Sitrep_No_09_Re_Magnitude_6_0_Earthquake_in_Wao_Lanao_Del_Sur_as_of_20April2017_8AM.pdf)
- 1106 National Structural Code of the Philippines (NSCP) (2015). *Buildings, Towers, And Other Vertical Structures*, Vol. 1.
1107 7th edition, Association of Structural Engineers of the Philippines, Inc.
- 1108 NPC (2015), *Nepal Earthquake 2015, Post Disaster Needs Assessment: Vol. A: Key Findings*, National Planning
1109 Commission, Government of Nepal.
- 1110 NRA (2018), “Rebuilding Nepal – Three years of construction”, A National Reconstruction Authority publication,
1111 Kathmandu, Nepal.
- 1112 OCHA, (2015), *Nepal: Earthquake 2015 Situation Report No. 17 (as of 21 May 2015)*
- 1113 OECD, (2017), *Protecting students and schools from earthquakes: The seven OECD principles for school seismic safety*.
1114 Secretary-General of the OECD
- 1115 Pazzia V., Morellia S., Pratesiab F., Sodía T., Valoric L., Gambaccianic L., Casaglia N., (2016), “Assessing the safety
1116 of schools affected by geo-hydrologic hazards: The geohazard safety classification (GSC)”, *International Journal of
1117 Disaster Risk Reduction*, Vol. 15, Pages 80-93.
- 1118 Racoma B.A.B., David C.P.C., Crisologo I.A., Bagtasa G., (2016), “The Change in Rainfall from Tropical Cyclones
1119 Due to Orographic Effect of the Sierra Madre Mountain Range in Luzon, Philippines.”, *Philippine Journal of Science*.
- 1120 Republic Act No. 10121, (2010), “An act strengthening the Philippine disaster risk reduction and Management system,
1121 providing for the national disaster risk Reduction and management framework and institutionalizing the National
1122 disaster risk reduction and management plan, Appropriating funds therefor and for other purposes.”, Republic of the
1123 Philippines Congress of the Philippines, Metro Manila.
- 1124 Rossetto T, Gehl P, Minas S, Galasso C, Duffour P, Douglas J, and Cook O (2016). *FRACAS: A capacity spectrum
1125 approach for seismic fragility assessment including record-to-record variability*. *Engineering Structures*, vol.125,
1126 pp.337–348.

Journal Pre-proof

1127 Sealza I, Sealza LP (2014). Recovering from the Effects of Natural Disaster: The Case of Urban Cagayan de Oro,
1128 Philippines. *European Journal of Sustainable Development*, 3(3):103-110.

1129 Seismosoft (2016). SeismoStruct v2016, A Computer Program for Static and Dynamic Nonlinear Analysis of Framed
1130 Structures.

1131 Shome, N., Cornell, C.A., Bazzurro, P., Carballo, J.E., 1998. Earthquakes, records, and nonlinear responses. *Earthq.*
1132 *Spectra* 14, 469–500.

1133 Shrestha, I N, 2018, Three years of school reconstruction, NRA Newsletter, issue 5, Nepal, 2018,
1134 <http://nra.gov.np/en/content/bulletins/0>

1135 Stephenson V, D'Ayala D (2014). A new approach to flood vulnerability assessment for historic buildings in England.
1136 *Natural hazards and Earth System Science*, 14:1035-1048. Takagi, H. & Esteban, M., (2016), "Statistics of tropical
1137 cyclone landfalls in the Philippines: unusual characteristics of 2013 Typhoon Haiyan", *Natural Hazards*, 80: 211.
1138 <https://doi.org/10.1007/s11069-015-1965-6>.

1139 The Guardian.(2009) ."Sichuan earthquake killed more than 5,000 pupils, says China". May 7, 2009. Available on line
1140 at <https://www.theguardian.com/world/2009/may/07/china-quake-pupils-death-toll>. (accessed on 01 July 2019)

1141 The World Bank (2019) Global Library of School Infrastructure (GLOSI), Global Program for Safer Schools (GPSS).
1142 Available online at: <https://gpss.worldbank.org/en/glosi> (accessed on 01 December 2019).

1143 UNDRR (2015), Sendai Framework for Disaster Risk Reduction 2015 - 2030, UN Office for Disaster Risk Reduction.
1144 Available online at https://www.unisdr.org/files/43291_sendaiframeworkfordrren.pdf (accessed on 01 July 2019).

1145 UNDRR (2017), Comprehensive School Safety, UN Office for Disaster Risk Reduction. Available online at
1146 https://www.preventionweb.net/files/31059_31059comprehensiveschoolsafetyframe.pdf (accessed on 01 July 2019).

1147 UNICEF (2018), Sulawesi Earthquake & Tsunami: One month on from the disaster, thousands of children still
1148 homeless, out-of-school and in need of humanitarian support [https://www.unicef.org.uk/press-releases/sulawesi-
1149 earthquake-tsunami-one-month-on-from-the-disaster-thousands-of-children-still-homeless-out-of-school-and-in-need-
1150 of-humanitarian-support/](https://www.unicef.org.uk/press-releases/sulawesi-earthquake-tsunami-one-month-on-from-the-disaster-thousands-of-children-still-homeless-out-of-school-and-in-need-of-humanitarian-support/) (accessed on 01 July 2019).

1151 UNISDR, (2014), "Comprehensive School Safety", United Nations Office for Disaster Risk Reduction (UNDRR).

1152 Verderame, G., Ricci, P., De Luca, F., Del Gaudio, C., & De Risi, M. T. (2014). Damage scenarios for RC buildings
1153 during the 2012 Emilia (Italy) earthquake. *Soil Dynamics and Earthquake Engineering*, 66, 385-400.
1154 <https://doi.org/10.1016/j.soildyn.2014.06.034>.

1155 Watt E., (2019), "When disaster strikes: how education and children's futures were battered by Cyclone Idai",
1156 Theirworld publications.

1157 WISS, (2013), "Worldwide Initiative for Safe Schools - Vision: By 2030, every school will be safe", United Nations
1158 Office for Disaster Risk Reduction (UNDRR).


1159 Wu, Y.F., Liu, T. and Oehlers, D.J (2006). Fundamental principles that govern retrofitting of reinforced concrete
1160 columns by steel and FRP jacketing, *Advances in Structural Engineering* 9(4): 507-533.

1161 Yamin, L.E., Rincón, J.R., Hurtado, Á.I., Becerra, A.F., Reyes J.C., López L.L., Dorado, J.F., Estrada, J., Cortez, F.R.,
1162 Atoche J.C., and Obando, L.D. (2015) la Evaluación del Riesgo Sísmico del Portafolio de Edificaciones En Locales
1163 Escolares del Perú a Partir De Los Resultados del CIE. Universidad de los Andes, Bogota, Columbia. (In Spanish)

1164 Yamin, L. E., Hurtado, A., Rincon, R., Dorado, J. F., & Reyes, J. C. (2017). Probabilistic seismic vulnerability
1165 assessment of buildings in terms of economic losses. *Engineering Structures*, 138, 308-323.

1166 INFORM (2019) Global Risk Index Results, European Union (EC), Inter-Agency Standing Committee
1167 (IASC).

**SAFER COMMUNITIES
THROUGH SAFER SCHOOLS
RAPID VISUAL SURVEY [v.3]**



General Info.	Date:	Time:	Surveyor Name:			
	School Compound Name / Address:					
	Building ID:		Total No. of Students in Building:			
	GPS Coordinate → Lat.:		Lon.:			
	Position → <input type="checkbox"/> Corner <input type="checkbox"/> Mid-block <input type="checkbox"/> End-block <input type="checkbox"/> Isolated <input type="checkbox"/> Other:					
	Construction Year:		<input type="checkbox"/> Unknown	Confidence: <input type="checkbox"/> H <input type="checkbox"/> M <input type="checkbox"/> L		
	Availability of Structural Drawing → <input type="checkbox"/> NO <input type="checkbox"/> YES Sketch a Simple Building Plan on the back of this Sheet					
	Any nearby Rivers → <input type="checkbox"/> NO <input type="checkbox"/> YES		Distance:			
	Any nearby Coasts → <input type="checkbox"/> NO <input type="checkbox"/> YES		Distance:			
	Any nearby Faults → <input type="checkbox"/> NO <input type="checkbox"/> YES		Distance:			
Building Info.	No. Storey :		Storey Height (m):			
	No. Bay X :		Total Length X (m):			
	No. Bay Y :		Total Length Y (m):			
	No. Rooms → Classroom:		Library:	Office:	IT Hub:	Hall: Services: Other:
	Dimension of Average Classroom (m) → X: Y:					
	Dimensions of Largest Room (m) → X: Y: Info:					
No. openings per storey:		Largest opening size (m):				
Structural Info.	Material of Load-Resisting System	<input type="checkbox"/> Masonry <input type="checkbox"/> Reinforced Concrete <input type="checkbox"/> Steel <input type="checkbox"/> Timber <input type="checkbox"/> Other:	<input type="checkbox"/>	Unk*	Confidence H M L	
	Floor Material	<input type="checkbox"/> RC Slab <input type="checkbox"/> Timber Joists + Wooden Floor <input type="checkbox"/> Reinforced Brick Concrete <input type="checkbox"/> Other:	<input type="checkbox"/>		H M L	
	Roof Structural System	<input type="checkbox"/> RC Slab <input type="checkbox"/> Timber Truss <input type="checkbox"/> Steel Truss <input type="checkbox"/> Reinforced Brick Concrete <input type="checkbox"/> Other:	<input type="checkbox"/>		H M L	
	Roof Covering	<input type="checkbox"/> Tiles <input type="checkbox"/> Metal Sheetting <input type="checkbox"/> Other:	<input type="checkbox"/>		H M L	
	Roof Pitch	<input type="checkbox"/> Flat <input type="checkbox"/> Mono Pitch <input type="checkbox"/> Multi Pitch → No.:	<input type="checkbox"/>		H M L	
	Roof Condition	<input type="checkbox"/> Poor/Deteriorated <input type="checkbox"/> Good/Fair <input type="checkbox"/> Excellent/Brand New	<input type="checkbox"/>		H M L	
	Roof Connection	<input type="checkbox"/> Poor/Deteriorated <input type="checkbox"/> Good/Fair <input type="checkbox"/> Excellent/Brand New	<input type="checkbox"/>		H M L	
	Lateral Load Resisting System	<input type="checkbox"/> Frame <input type="checkbox"/> Load Bearing Walls <input type="checkbox"/> RC Shear Wall <input type="checkbox"/> Bracing <input type="checkbox"/> Confined Masonry <input type="checkbox"/> Reinforced Masonry <input type="checkbox"/> Combined <input type="checkbox"/> Other:	<input type="checkbox"/>		H M L	
	Structural Condition	<input type="checkbox"/> Poor/Deteriorated <input type="checkbox"/> Good/Fair <input type="checkbox"/> Excellent/Brand New	<input type="checkbox"/>		H M L	
	Connection Quality	<input type="checkbox"/> Poor/Deteriorated <input type="checkbox"/> Good/Fair <input type="checkbox"/> Excellent/Brand New	<input type="checkbox"/>		H M L	
	Retrofitting	<input type="checkbox"/> No <input type="checkbox"/> Yes → Info:	<input type="checkbox"/>		H M L	
	Modifications	<input type="checkbox"/> No <input type="checkbox"/> Yes → Info: Addition of Stories: Extension of Plan:	<input type="checkbox"/>		H M L	
	Foundation Type	<input type="checkbox"/> RC <input type="checkbox"/> Brick <input type="checkbox"/> Stone <input type="checkbox"/> Other	<input type="checkbox"/>		H M L	
	Vulnerability Factors (Indicate Confidence)	<input type="checkbox"/> Short column <input type="checkbox"/> Pounding (if buildings closer than 0.2m) <input type="checkbox"/> Soft storey <input type="checkbox"/> Strong Beam-Weak Column <input type="checkbox"/> Built on Slope <input type="checkbox"/> Built on Stilts <input type="checkbox"/> Balconies <input type="checkbox"/> Plan irreg. <input type="checkbox"/> Elevation irreg. <input type="checkbox"/> Mass irreg. <input type="checkbox"/> Opening irreg. <input type="checkbox"/> Parapet <input type="checkbox"/> Gable <input type="checkbox"/> Other:				
	IF MASONRY:					
Masonry Type	<input type="checkbox"/> Masonry Brick <input type="checkbox"/> Masonry Block <input type="checkbox"/> Concrete Block <input type="checkbox"/> Cut stone <input type="checkbox"/> Adobe <input type="checkbox"/> Rubble Stone <input type="checkbox"/> Other	<input type="checkbox"/>			H M L	
Mortar Type	<input type="checkbox"/> None <input type="checkbox"/> Cement <input type="checkbox"/> Lime <input type="checkbox"/> Mud	<input type="checkbox"/>			H M L	
Reinforcement	<input type="checkbox"/> No <input type="checkbox"/> Yes	<input type="checkbox"/>			H M L	
Confinement	<input type="checkbox"/> No <input type="checkbox"/> Yes	<input type="checkbox"/>			H M L	
Wall Thickness (m)		<input type="checkbox"/>			H M L	
Wall Layer	<input type="checkbox"/> Solid <input type="checkbox"/> Multi Leaf <input type="checkbox"/> Cavity Walls	<input type="checkbox"/>			H M L	
IF FRAME [RC, Timber, Steel]:						
Beam Dimensions (m)		<input type="checkbox"/>			H M L	
Column Dimensions (m)		<input type="checkbox"/>			H M L	
Infill Wall Material	<input type="checkbox"/> Brick <input type="checkbox"/> Concrete Block <input type="checkbox"/> Timber Plates <input type="checkbox"/> Adobe <input type="checkbox"/> Other: Thickness (m):	<input type="checkbox"/>			H M L	

*Unknown H = high, M = medium, L = low Any extra comments can be added on the back of this sheet.

© 2017 EPICentre®
Prepared by: Arash Nassirpour, Rohit Kumar Adhikari,
Carmine Galasso & Dina D'Ayala






Figure A-1. SCOSSO rapid visual survey data collection form

Declaration of interests

The authors declare that they have no known competing financial interests or personal relationships that could have appeared to influence the work reported in this paper.

The authors declare the following financial interests/personal relationships which may be considered as potential competing interests: